BM@N Analysis Note
Production of *p, d, t* in 3.2 A GeV argon-nucleus interactions

Analysis team: M.Kapishin, L.Kovachev, V.Plotnikov, Yu.Petukhov, I.Rufanov, A.Zinchenko

Abstract

Production of *p, d, t* in interactions of the argon beam with the kinetic energy 3.2 AGeV with the *C, Al, Cu, Sn, Pb* targets was studied with the BM@M detector at the Nuclotron. The analysis procedure is described in details. Results on *p, d, t* yields have been obtained and compared with model predictions and data available.

Event reconstruction

The track reconstruction method was based on the so-called "cellular automaton" approach [CBM1]. The tracks found were used to reconstruct primary and secondary vertices using the "KF-particle" formalism [CBM2]. *p, d, t* were identified using the time of flight from the ToF detectors, the length of the trajectory and the momentum reconstructed in the central tracker. The *p, d, t* candidates should originate from the primary event vertex, correlate with hits in the CSC / DCH detectors and match hits in the ToF-400 / ToF-700 detectors. Herewith, the CSC (DCH) hits were used to confirm the quality of the tracks matched to ToF-400 (ToF-700) hits. Events were recorded with different conditions on the minimum number of fired channels in the barrel BD and multiplicity silicon SiMD trigger detectors, ranging from zero to 4.

Table 1a. Number of triggered events, beam fluxes and integrated luminosities collected in interactions of the argon beam of 3.2 AGeV with different targets (ToF-400 data sample).

Interactions, target thickness	Number of triggers / 10^6	Integrated beam flux / 10^7	Integrated luminosity / 10^{30} cm^{-2}
Ar+C (2 mm)	9.5	9.1	2.06
Ar+Al (3.33 mm)	24.1	11.5	2.30
Ar+Cu (1.67 mm)	24.5	12.7	1.79
Ar+Sn (2.57 mm)	23.8	11.6	1.11
Ar+Pb (2.5 mm)	11.7	6.1	0.50

Table 1b. Number of triggered events, beam fluxes and integrated luminosities collected in interactions of the argon beam of 3.2 AGeV with different targets (ToF-700 data sample).

Interactions, target thickness	Number of triggers / 10^6	Integrated beam flux / 10^7	Integrated luminosity / 10^{30} cm^{-2}
Ar+C (2 mm)	9.4	8.7	1.97
Ar+Al (3.33 mm)	21.6	10.2	2.05
Ar+Cu (1.67 mm)	21.0	11.3	1.60

Ar+Sn (2.57 mm)	19.0	9.5	0.91
Ar+Pb (2.5 mm)	9.7	4.9	0.40

***p, d, t* selection criteria:**

- Each track has at least 4 hits in GEM detectors (6 detectors in total), where hit is a combination of two strip clusters on both readout sides (*X* and *X′* views) on each detector [GEMTDR]
- Tracks are originated from the primary event vertex, the deviation of the reconstructed vertex from the position of the target along the beam direction $-3.4<|Z_{vertex} - Z_0|<1.7$ cm. A harder upper limit is aimed to remove background due to interactions in a scintillator counter behind the target.
- Distance of the closest approach of tracks from the vertex in the direction perpendicular to the beam at Z_{vertex}: dca < 1 cm
- $\chi 2$ / ndf for tracks from the primary vertex < 3.5^2
- Momentum range of positive tracks: $p_{pos}>0.5$, 0.7 GeV/*c* for analysis of the ToF-400 and ToF-700 data, respectively
- Correlation of extrapolated tracks with the CSC / DCH hits as well as with the ToF-400 / ToF-700 hits should be within ±2.5σ of the residual distributions.

Event simulation:

The Monte Carlo event samples of *Ar+A* collisions were produced with the DCM-SMM event generator. The passage of particles through the setup volume was simulated with the GEANT program integrated into the BmnRoot software framework. To properly describe the GEM detector response in the magnetic field, the microsimulation package Garfield++ was used. The package gives very detailed description of the processes inside the GEM detector, including the drift and diffusion of released electrons in electric and magnetic fields and the electron multiplication in GEM foils, so that the output signal from the readout plane can be reproduced. To speed up the simulation, dependencies of the Lorentz shifts and the charge distributions on the readout planes on the drift distance were parameterized and used in the GEM digitization part of the BmnRoot package. The details of the detector alignment, Lorenz shift corrections are described in the paper [DeuteronPaper]. Examples of experimental and Monte Carlo distributions of the distance of the closest approach of tracks to the vertex, χ^2 of reconstructed tracks, number of tracks reconstructed in the primary vertex, number of hits per track are presented in Fig.3a. The detector effects in simulation were controlled by reproducing the track reconstruction efficiency evaluated from data. Efficiency distributions in 3 Si and 6 GEM stations were measured with reconstructed experimental tracks. For each station they were estimated using the following approach:

1. Select good quality tracks with the number of hits per track (excluding the station under study) not less than *N*;
2. Check that track crosses the detector area, if yes, add one track to the denominator;
3. If there is a hit in the detector, which belongs to the track, add one track to the numerator;
4. Detector efficiency is equal to the ratio of number of tracks in numerator to number of tracks in denominator.

These efficiencies were applied to reduce the number of hits of tracks reconstructed in simulation. Details of the adjustment of the simulated distributions to the data are described in [NotePi+K+].

Signals of *p, d, t* in experimental data:

The mass squared spectrum of positive particles identified in ToF-400 and ToF-700 in experimental events of *Ar+A* interactions are illustrated in Fig.10a and 10b, respectively. Signals of *p, d, t* were extracted in windows of the mass squared from 0.4 to 1.5 $(GeV/c^2)^2$, 2.4 to 4.8 $(GeV/c^2)^2$ and 6.6 to 9.6 $(GeV/c^2)^2$, respectively. The precise widths of the mass squared windows are dependent on the transverse momentum p_T and rapidity y_{lab}. Numbers of *p, d, t* were taken from the content of the histogram bins within the corresponding mass squared windows. The histograms were filled in the intervals of the transverse momentum p_T and rapidity y_{lab}. To estimate the background in the *p, d, t* mass squared windows, the distributions were fitted to the 1st degree polynomial (linear fit). The *p, d, t* mass squared peak ranges were excluded from the fit. The errors of the *p, d, t* signals include the uncertainty of the background subtraction. The statistical errors were calculated according to the formula: $sig = hist - bg$, $err(stat) = \sqrt{hist + bg}$, assuming the background uncertainty of $\sqrt{bg}$. Here *hist* and *bg* denote the histogram integral and the background integral within the *p, d, t* mass squared windows. As examples, the data and simulated spectra of the mass squared of *deuterons* identified in ToF-700 in Ar+Sn interactions are shown in Fig.10c and 10d in bins of the rapidity y_{lab}.. The data spectra of *tritons* identified in ToF-700 are shown in Fig.10e in bins of the rapidity y_{lab}. Plots in Fig.10c-e illustrate the background subtraction method using the linear fit. Bins with zero errors in the mass squared peak ranges were excluded from the fit. The “mixed event” method reproduces smooth behavior of the background and gives results consistent to the linear fit, The difference is found to be within the background uncertainty of $\sqrt{bg}$.

Statistics of *p, d, t* reconstructed in ToF-400 and ToF-700 in *Ar+C, Ar+Al, Ar+Cu, Ar+Sn, Ar+Pb* interactions are summarized in Table 2. Number of reconstructed *p, d, t* in Ar+Sn interactions in bins of y_{lab} and p_T are shown in Fig. 11a (11b) for ToF-400 (ToF-700) data. In Fig.11c-11e data spectra on y_{lab} and p_T for *p, d, t* identified in ToF-400 and ToF-700 are compared with the simulated DCM-SMM spectra. The corresponding 2-dimensional (y_{lab}, p_T) data distributions for *p, d, t* identified in ToF-400 and ToF-700 are shown in Fig.11f and 11g.

Table 2. Statistics of *p, d, t* identified in ToF-400 and ToF-700 in argon-nucleus interactions. The errors present statistical uncertainties.

Target	***ToF-400***				
	C	***Al***	***Cu***	***Sn***	***Pb***
Protons	237300±1100	787900±1800	750200±1500	643000±1300	373000±900
Deuterons	18900±340	71300±680	70100±550	64600±440	38100±300
Tritons	750±80	3970±150	3990±140	4170±120	2980±80
Target	***ToF-700***				

	C	*Al*	*Cu*	*Sn*	*Pb*
Protons	216100±1300	640400±1900	611100±1600	635100±1400	291700±900
Deuterons	31200±700	101200±1100	88300±730	91900±640	41800±380
Tritons	1180±120	4430±200	4560±170	6000±150	3190±90

p,/ d, t reconstruction efficiency from simulation:

The p, d, t reconstruction efficiency is the ratio of the number of reconstructed p / d / t to the number of generated ones in the intervals of (p_T,y), where y is measured in the laboratory frame (y_{lab}). The reconstruction efficiency can be decomposed into the following components: $\varepsilon_{rec} = \varepsilon_{acc} \cdot \varepsilon_{cuts}$.. The definition of every term is given in Table 4 and their determination procedure is as follows. After the event simulation and reconstruction the successfully reconstructed p / d / t were counted in the numerator N_{acc}. The detector acceptance was taken as N_{acc} / N_{gen}, where N_{gen} is the total number of generated MC events. The number of p / d / t after applying kinematic and spatial cuts (N_{cuts}) gave the "selection cuts" efficiency with respect to the number of accepted ones from above.

Table 4. Decomposition of the p / d / t reconstruction efficiency.

Reconstruction efficiency	$\varepsilon_{rec} = \varepsilon_{acc} \cdot \varepsilon_{cuts}$
p / d / t geometrical acceptance in detectors	$\varepsilon_{acc} = N_{acc} (y,p_T) / N_{gen} (y,p_T)$
Efficiency of reconstruction of p/ d / t within the detector geometrical acceptance after applying kinematic and spatial cuts	$\varepsilon_{cuts} = N_{cuts}(y,p_T) / N_{acc}(y,p_T)$

The actual values of the reconstruction efficiency ε_{rec} calculated in the y, p_T bins and 2-dimensional (y, p_T) bins are shown in Figs. 12a and 12b for p, d, t identified in ToF-400 and ToF-700 in *Ar+Sn* interactions.

Trigger efficiency:

The trigger efficiency ϵtrig depends on the number of fired channels in the BD (SiMD) detectors. It was calculated for events with reconstructed protons, deuterons, tritons using event samples recorded with an independent trigger based on the SiMD (BD) detectors. The BD and SiMD detectors cover different and non-overlapping regions of the BM@N acceptance, that is, they detect different collision products. For the BD trigger efficiency estimation, the following relation is used: ϵtrig (BD ≥ m) = N(BD ≥ m ∧ SiMD ≥ n)/N(SiMD ≥ n), where m and n are the minimum number of fired channels in BD (m = 3, 4) and SiMD (n = 3, 4). A similar relation is used to evaluate the SiMD trigger efficiency. The BD (SiMD) trigger efficiency is averaged over all data with the different values of the minimum number of fired channels in SiMD (BD). The efficiency of the combined BD and SiMD triggers was calculated as the product of the efficiencies of the BD and SiMD triggers. The trigger efficiency evaluated in events with reconstructed protons, deuterons, tritons was found to be consistent.

The mean efficiency ε_{trig} of the BD and SiMD trigger detectors was measured in events with reconstructed *p / d / t* produced in interactions of the argon beam with sets of data with the *C, Al, Cu, Sn, Pb* targets. The results for the BD and SiMD detectors are given in Table 5a and 5b, respectively. The dependence of the BD and SiMD trigger efficiency on the number of tracks from the primary vertex for events with reconstructed *p , d , t* is presented in Fig.13a and 13b, respectively. The systematic errors used in the analysis cover the differences in the *p, d, t* signals obtained by using the mean values of the trigger efficiency values instead of the efficiency dependences on the number of the vertex tracks and the Y position of the primary vertex.

Table 5a. Mean BD trigger efficiency evaluated for events with reconstructed *p / d / t* in interactions of the argon beam with the *C, Al, Cu, Sn, Pb* targets.

Trigger / Target 3.2 AGeV *p/d /t*	***C***	***Al***	***Cu***	***Sn***	***Pb***
ε_{trig} (BD)	0.54±0.03	0.86±0.01	0.93±0.01	0.95±0.01	0.95±0.01

Table 5b. Mean SiMD trigger efficiency evaluated for events with reconstructed *p / d / t* in interactions of the argon beam with the *C, Al, Cu, Sn, Pb* targets.

Trigger / Target 3.2 AGeV *p/d /t*	***C***	***Al***	***Cu***	***Sn***	***Pb***
ε_{trig} (SiMD)	0.13±0.03	0.20±0.02	0.34±0.02	0.44±0.01	0.52±0.01

Luminosity uncertainty (see document [Lumi])

Selection of the centrality classes (see document [Centrality])

Evaluation of *p / d / t* cross sections and spectra:

The differential cross sections $d^2\sigma_{p,d,t}\ (y,p_T)/dydp_T$ and multiplicities $d^2N_{p,d,t}(y,p_T)/dydp_T$ of proton, deuteron, triton production in Ar+C, Al, Cu, Sn, Pb interactions are calculated using the relations:

$$d^2\sigma_{p,d,t}\ (y,p_T)/dydp_T = \ \Sigma\ [\ d^2n\ p,d,t\ (y,p_T,\ N_{tr})\ /\ (\varepsilon_{trig}(N_{tr})\ dy\ dp_T)]\ \cdot\ 1\ /\ (\ L\ \varepsilon_{rec}\ (y,p_T))$$

$$d^2N_{p,d,t}\ (y,p_T)/dydp_T = d^2\sigma_{p,d,t}\ (y,p_T)\ /\ (\sigma_{inel}\ dydp_T) \qquad (1)$$

where the sum is performed over bins of the number of tracks in the primary vertex, N_{tr}, $n_{p,d,t}\ (y, p_T, N_{tr})$ is the number of reconstructed protons, deuterons, tritons in the intervals dy and dp_T (Fig.11f,g) , $\varepsilon_{trig}\ (N_{tr})$ is the track-dependent trigger efficiency (Fig.13a,b), ε_{rec} is the reconstruction efficiency of protons, deuterons, tritons (Fig.12a,b), L is the luminosity (Table 1), and σ_{inel} is the inelastic cross section for argon-nucleus interactions (Table 11).
The cross sections in (y, p_T) bins are calculated as weighted averaged of the results obtained with ToF-400 and ToF-700 data taking into account the statistical errors (w ~ $1/\sigma^2$).

Systematic uncertainties:

Table 10 summarizes the mean values, averaged over p_T, y and N_{tr}, of the systematic uncertainties of the various factors of Eq. (1), $n_{p,d,t}$, ε_{rec} and ε_{trig}. Details are given below, including the uncertainty of the luminosity measurement. The model uncertainty of σ_{inel} is given in Table 11. Several sources are considered for the evaluation of the systematic uncertainty of the proton, deuteron, triton yield, $n_{p,d,t}$ and the reconstruction efficiency ε_{rec}. The most significant ones are discussed below. Some of them affect both the yield $n_{p,d,t}$ and the reconstruction efficiency, ε_{rec}. For these cases the correlated effect is taken into account by the variations on the $n_{p,d,t} / \varepsilon_{rec}$ ratio:

- Systematic uncertainty of the central tracking detector efficiency: it is estimated from the remaining difference in the number of track hits in the central detectors in the simulation relative to the data (see Fig. 3a, low right plot) and found to be within 3%.
- Systematic uncertainty of the matching of central tracks to the CSC (DCH) hits and ToF-400 (ToF-700) hits: it is estimated from the remaining difference in the matching efficiency in the simulation relative to the data and found to be within 5%.
- Systematic uncertainty of the reconstruction efficiency due to the remaining difference in the X/Y distribution of primary vertices, the beam tilt and angular spread in the simulation relative to the data.
- Systematic uncertainty of the background subtraction in the mass-squared M^2 spectra of identified particles: it is estimated as the background integral $\sqrt{bg}$ from the fitting of the M^2 spectra by a linear function. The latter is done in the M^2 range with excluding the proton, deuteron, triton windows (see section **Signals of *p, d, t* in experimental data).**
- Uncertainy ot the centrality class selection estimated as a fraction of events migrated from the centrality class 40-100% to the centrality class 0-40% and vice versa (see document [Centrality]).

The total systematic uncertainty of the yield and reconstruction efficiency for the various targets, calculated as the quadratic sum of these uncertainties, is listed in Table 10. The luminosity is calculated from the beam flux ϕ as given by the beam trigger (see section **Trigger efficiency** and document [TriggerEff]) and the target thickness l using the relation: $L = \phi\rho l$ where ρ is the target density expressed in atoms/cm3. The systematic uncertainty of the luminosity is estimated from the fraction of the beam which can miss the target, determined from the vertex positions, and found to be within 2%.

For the evaluation of the systematic uncertainty of the trigger efficiency ϵ_{trig}, the following sources are considered:

- The systematic uncertainty associated with the factorization assumption of the two trigger factors, BD and SiMD, was estimated from the difference of ϵtrig evaluated as described in section **Trigger efficiency**, with the result evaluated using the limited amount of events registered with the beam trigger BT.
- To estimate a possible distortion of ϵtrig (BD ≥ m) due to the selection of events with the hardware-set condition N(SiMD ≥ n), ϵ_{trig} was also evaluated using the events recorded with the beam trigger BT. The difference between the results is treated as another source of systematic uncertainty of the trigger efficiency.
- Variations of the trigger efficiency on the track multiplicity in the primary vertex and on the X/Y vertex position.

The total systematic uncertainty of the trigger efficiency for the various targets, calculated as the quadratic sum of these uncertainties, is listed in Table 10b.

The normalization uncertainty of the trigger efficiency is 28% for *d, t* detection in Ar+C interactions and between 7.5% (Ar+Al) and 4% (Ar+Pb) for *d, t* detection in interactions of argon with more heavy targets. The trigger efficiency uncertainty for *p* detection ranges between 4.5% (Ar+C) and 0.9% (Ar+Pb). The mean values of systematic uncertainties *p,d,t* yields in Ar+C, Al, Cu, Sn, Pb interactions are summarized in Table 10.

Table 10. Systematic uncertainty of the *p,d,t* yields measured argon-nucleus interactions in centrality ranges 0-40% and 40-100%.

Target / Systematics		*p/d/t, 0-40%*				Target		*p/d/t, 40-100%*			
	C sys%	***Al*** sys%	***Cu*** sys%	***Sn*** sys%	*Pb* sys%		***C*** sys%	***Al*** sys%	***Cu*** sys%	***Sn*** sys%	***Pb*** sys%
Sys total	14	12	12	10	10		28	26	14	12	16
Norm (trigger + tracking + luminosity)	10	7	7	7	7		10	7	7	7	7

The cross sections for inelastic *Ar+Al, Ar+Cu, Ar+Sn, Ar+Pb* interactions are taken from the predictions of the DCM-SMM model which are consistent with the results calculated by the formula: $\sigma_{inel} = \pi R_0^2 (A_P^{1/3} + A_T^{1/3})^2$, where R_0 = 1.2 fm is an effective nucleon radius, A_P and A_T are atomic numbers of the beam and target nucleus. The uncertainties for *Ar+Al, Ar+Cu, Ar+Sn, Ar+Pb* inelastic cross sections are estimated by using the alternative formula: $\sigma_{inel} = \pi R_0^2 (A_P^{1/3} + A_T^{1/3} - b)^2$ with R_0 = 1.46 fm and b = 1.21 [AngelovCC].

Table 11. Inelastic cross sections for argon-nucleus interactions.

Interaction	***Ar+C***	***Ar+Al***	***Ar+Cu***	***Ar+Sn***	***Ar+Pb***
Inelastic cross section, mb	1470±50	1860±50	2480±50	3140±50	3970±50

The yields of *p / d / t* in minimum bias *Ar+C, Ar+Al, Ar+Cu, Ar+Sn, Ar+Pb* interactions are measured in the kinematic range on the transverse momentum of $0.1<p_T<1.2$ GeV/*c* for *p* ($0.15<p_T<1.45$ GeV/*c* for *d* and $0.2<p_T<1.6$ GeV/*c* for *t*) and the rapidity in the laboratory frame of $0.9<y_{lab}<2.5$ for *p* ($0.7<y_{lab}<2.3$ for *d* and $0.6<y_{lab}<2.0$ for *t*). The rapidity of the beam-target nucleon-nucleon CM system calculated for an interaction of the argon beam with the kinetic energy of 3.2 GeV/nucleon with a fixed target is y_{CM}=1.08. The transformation of the *y* distribution to c.m.s. gives $y^*=y_{lab}-y_{CM}$. The differential y_{lab} spectra of *p* yields for centralities 0-40% and 40-100% are presented in Figs. 15a and 15b, respectively. The corresponding differential y_{lab} spectra of *d* and *t* yields are presented in Fig.15c-15f. Predictions of the DCM-SMM model are shown for comparison. The corrected invariant differential p_T spectra of *p, d, t* yields for centralities 0-40% and 40-100% are presented in Fig. 16a-f. The measured spectra of the *p, d, t* yields in p_T are parameterized by the form: $1/m_T \cdot d^2Y/dm_T dy\ N \cdot m_T \cdot exp(-(m_T-m)/T)$, where $m_T=\sqrt{(m^2+p_T^2)}$ is the transverse mass of *p, d, t*. The normalization *N* and the inverse slope parameter *T* are free parameters of the fit, interval *dy* corresponds to the measured y_{lab} range. In

Fig.17a-17c the inverse slopes *T* of the experimental invariant p_T spectra of p / d / t are presented for intervals of rapidity y_{lab}. The experimental results are compared with predictions of the DCM-SMM model.

Summary

Production of *p, d, t* in interactions of the argon beam with *C, Al, Cu, Sn, Pb* targets was studied with the BM@N detector. The analysis procedure is described including details of the *p, d, t* reconstruction, efficiency and systematic uncertainty evaluation. First physics results are presented on *p, d, t* yields in argon-nucleus interactions for centralities of 0-40% and 40-100% at the beam kinetic energy of 3.2 AGeV. The results are compared with models of nucleus-nucleus interactions.

Bibliography

[DeuteronPaper] D.Baranov et al., First Results from BM@N Technical Run with Deuteron Beam, Phys. Part. Nucl. Lett. 15, no. 2, 148 (2018)

[GEMconf] https://bmn-wiki.jinr.ru/bin/view/Run/2.%20Run%20Control/2.1%20Run%207/BM%40N%20Session%20%28GEM%29/

[GEMTDR] https://bmn-wiki.jinr.ru/bin/view/Doc/4.%20Documents/4.4%20BM%40N%20TDR/GEM%20tracker/

[CBM1] V. Akishina and I. Kisel. Time-based cellular automaton track finder for the CBM experiment - 2015. J. Phys.: Conf. Ser. 599, 012024

[CBM2] S. Gorbunov and I. Kisel. Reconstruction of decayed particles based on the Kalman filter - 2007. CBM-SOFTnote--003

[NotePi+K+]

[TriggerEff]

[Lumi]

[Centrality]

[AngelovCC] H.Angelov et al., P1-80-473, JINR, Dubna

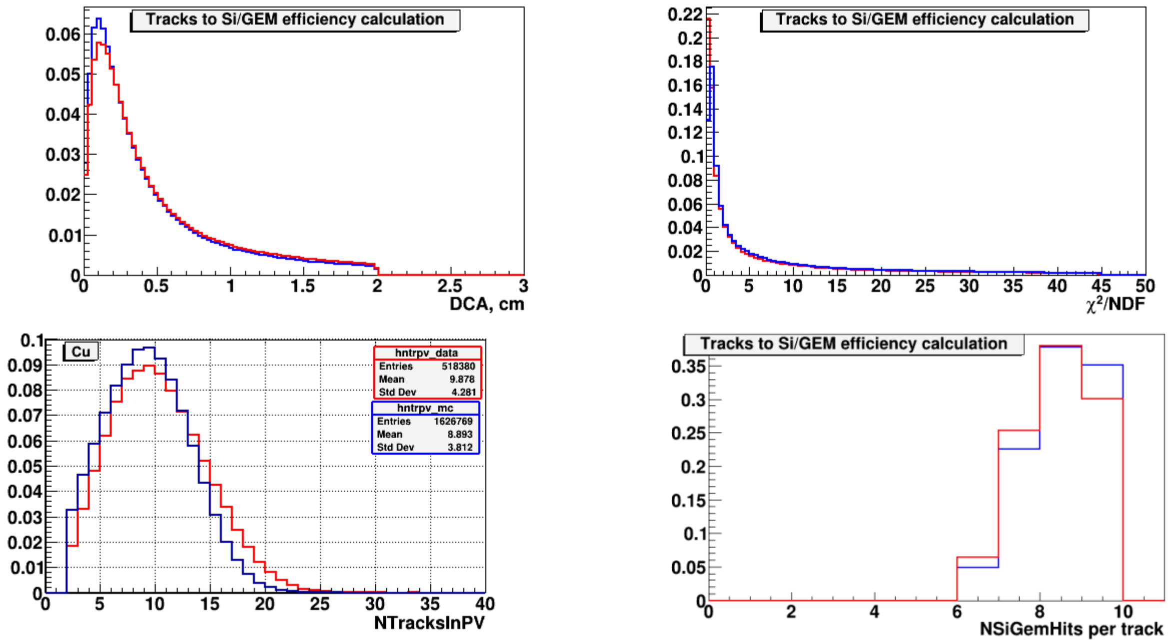

Fig.3a. *Ar+A* interactions at 3.2 AGeV argon beam energy: comparison of experimental distributions (red lines) and Monte Carlo GEANT distributions of events generated with the DCM-SMM model (blue lines): Distribution of the distance of the closest approach DCA between tracks and the vertex in the plane perpendicular to the beam direction; χ^2 of reconstructed tracks; number of tracks reconstructed in the primary vertex; number of hits per track reconstructed in 3 Si + 6 GEM detectors.

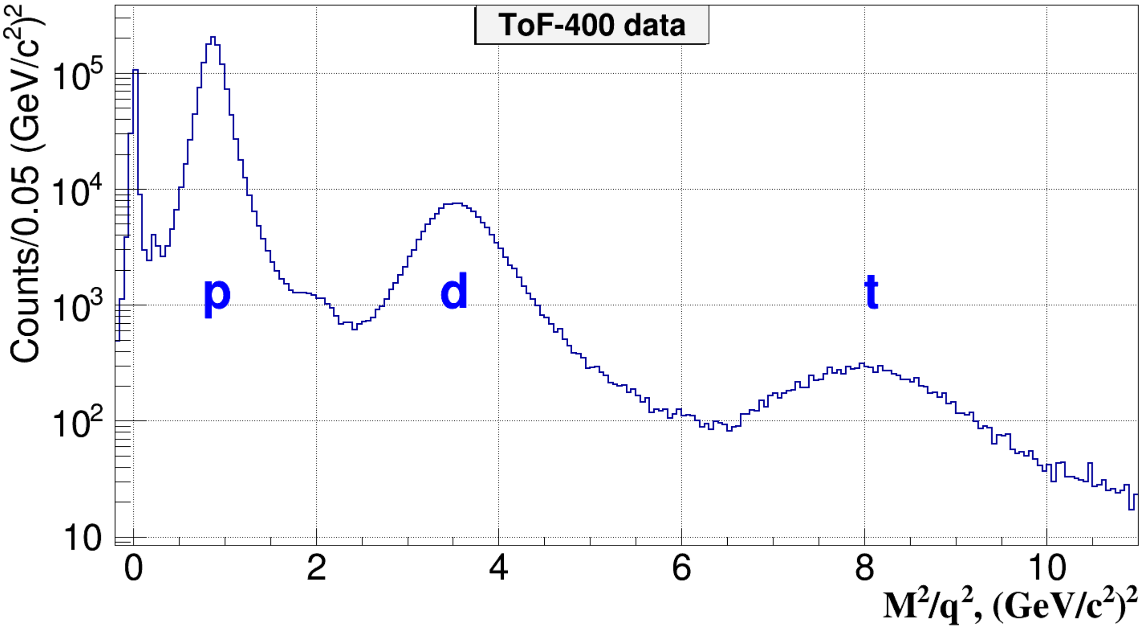

Fig. 10a. Data spectrum of mass squared of particles identified in ToF-400 in *Ar+A* interactions: signals of protons, deuterons and tritons are shown.

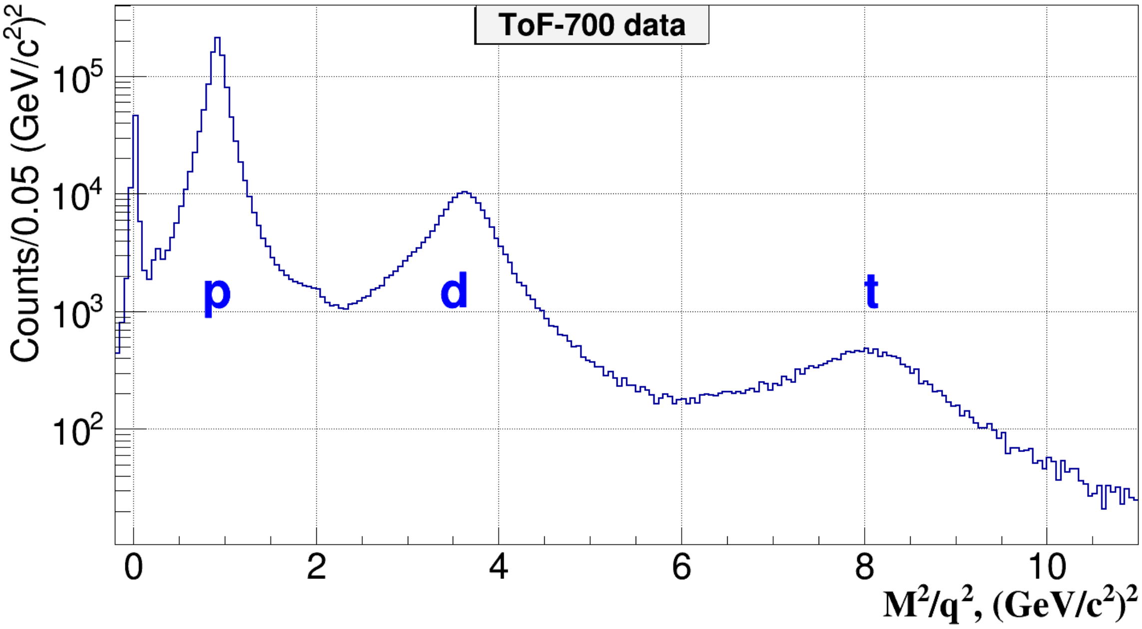

Fig. 10b. Data spectrum of mass squared of particles identified in ToF-700 in Ar+A interactions: signals of protons, deuterons and tritons are shown.

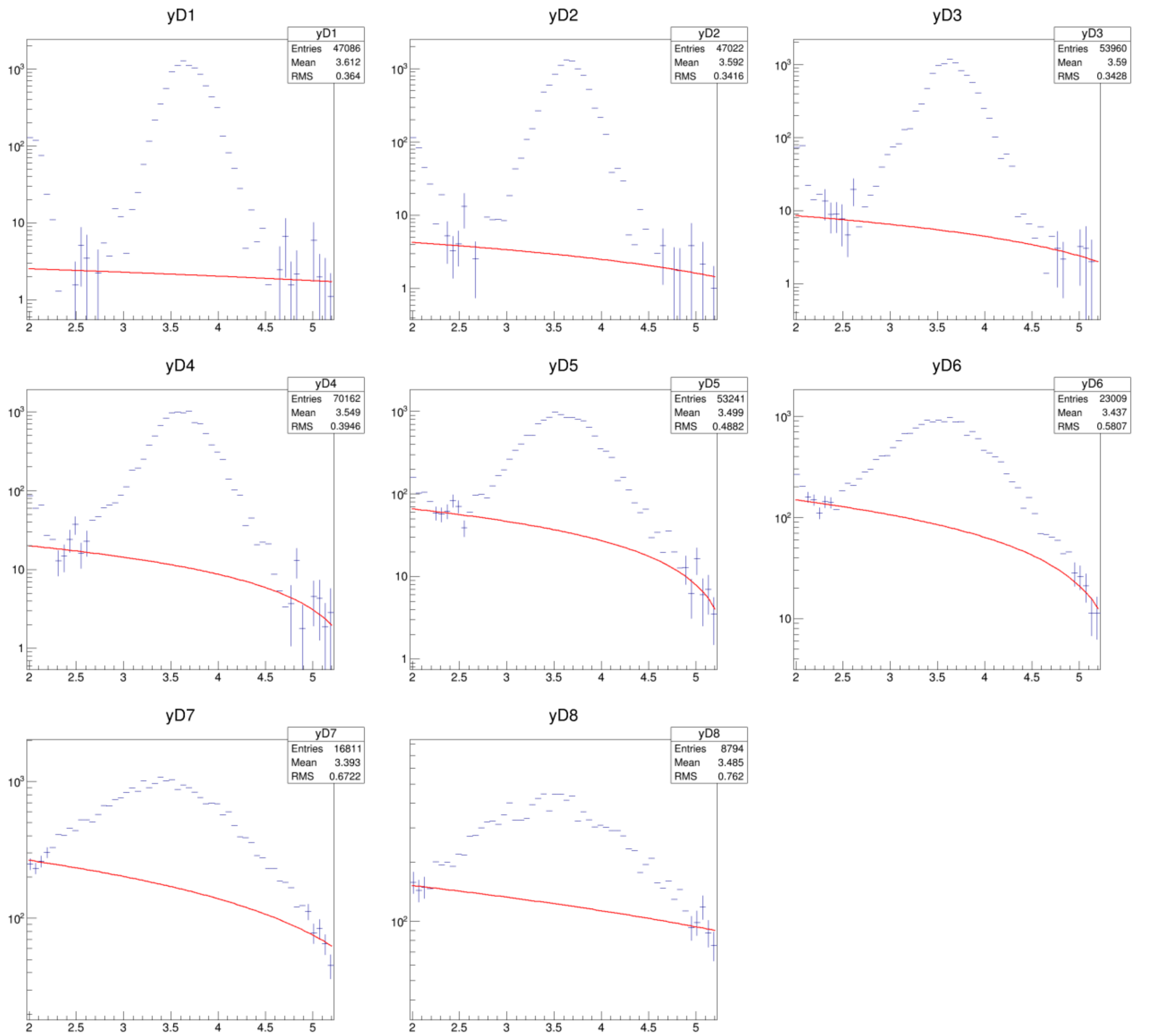

Fig. 10c. Data spectrum of mass squared in bins of y_{lab} of *deuterons* identified in ToF-700 in Ar+Sn interactions: background subtraction by the linear fit is described in the text.

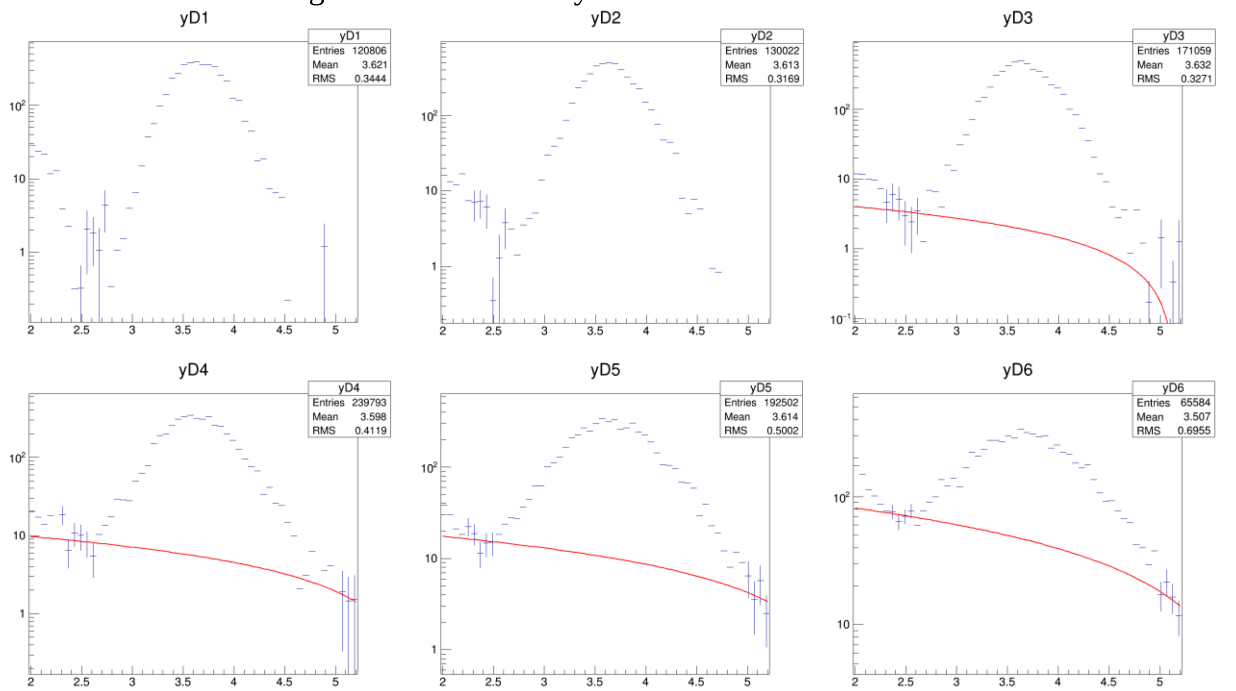

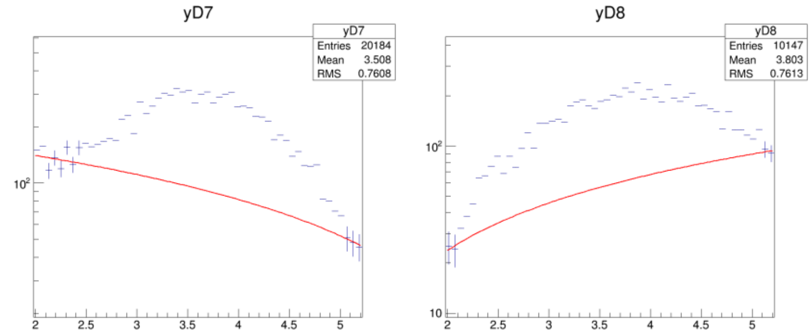

Fig. 10d. Simulated spectrum of mass squared in bins of y_{lab} of *deuterons* identified in ToF-700 in Ar+Sn interactions: background subtraction by the linear fit is described in the text.

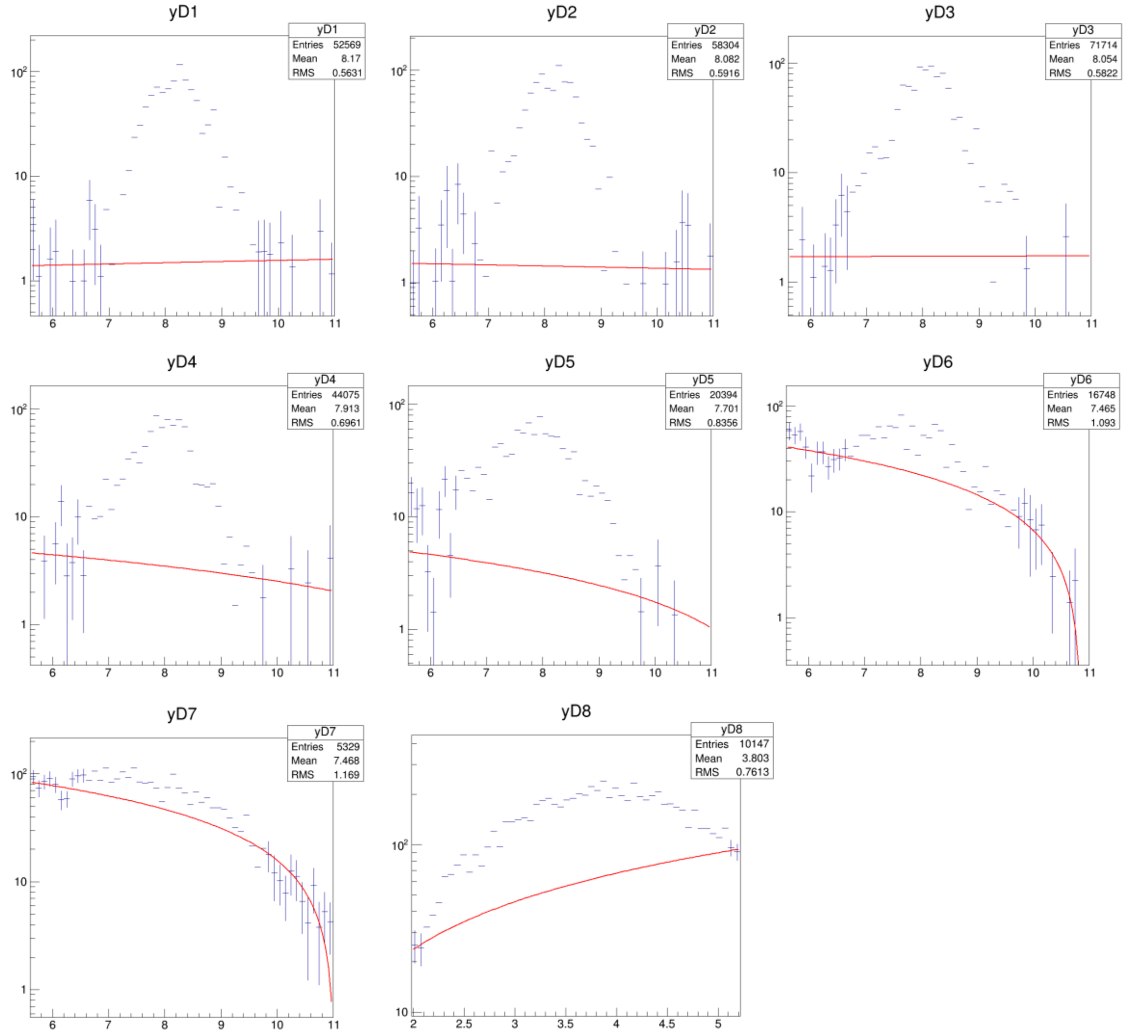

Fig. 10e. Data spectrum of mass squared in bins of y of *tritons* identified in ToF-700 in Ar+Sn interactions: background subtraction by the linear fit is described in the text.

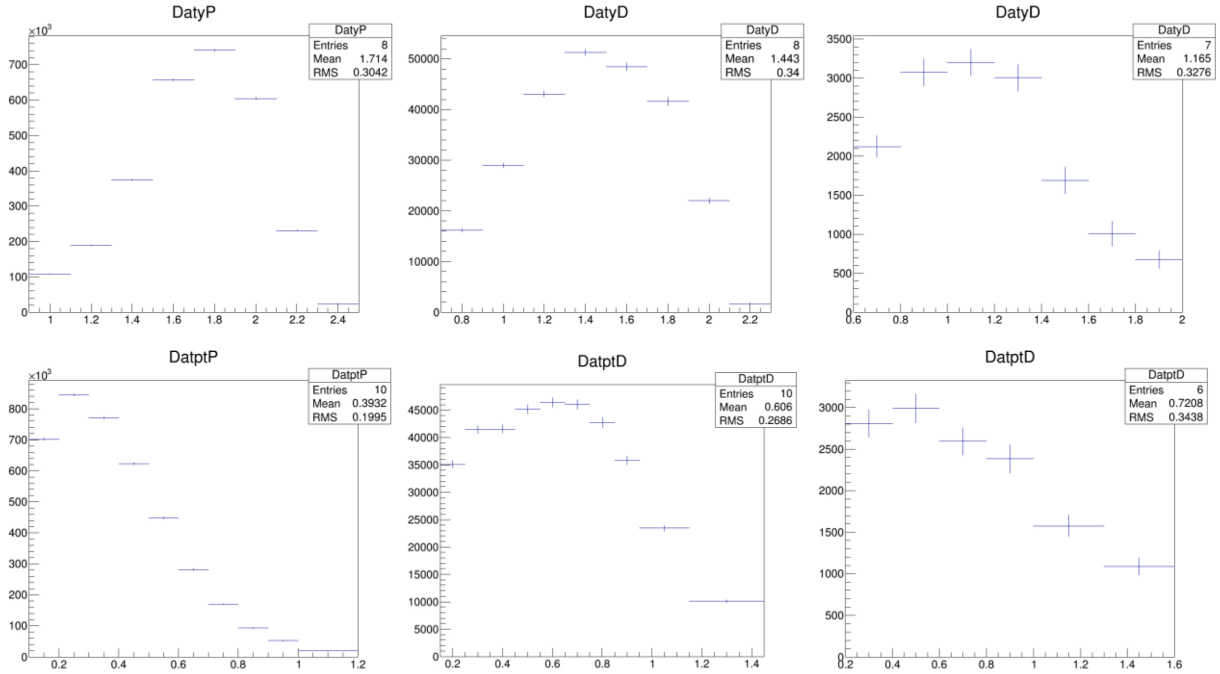

Fig.11a. Data spectrum of *protons (left), deuterons (center), tritons (right)* identified in ToF-400 in Ar+Sn interactions in bins of y_{lab} (upper plots) and p_T (lower plots).

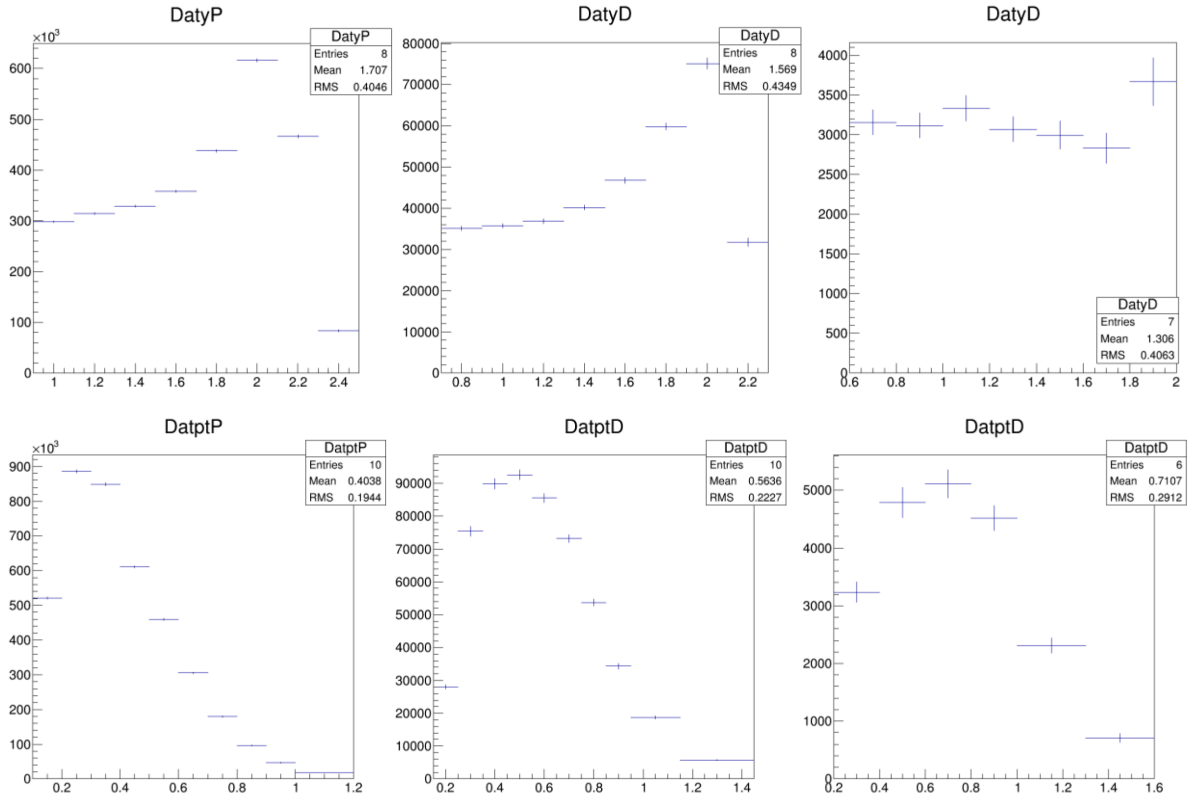

Fig.11b. Data spectrum of *protons (left), deuterons (center), tritons (right)* identified in ToF-700 in Ar+Sn interactions in bins of y_{lab} (upper plots) and p_T (lower plots).

ToF-400 Sim / Data proton y spectrum ToF-700 Sim / Data proton y spectrum

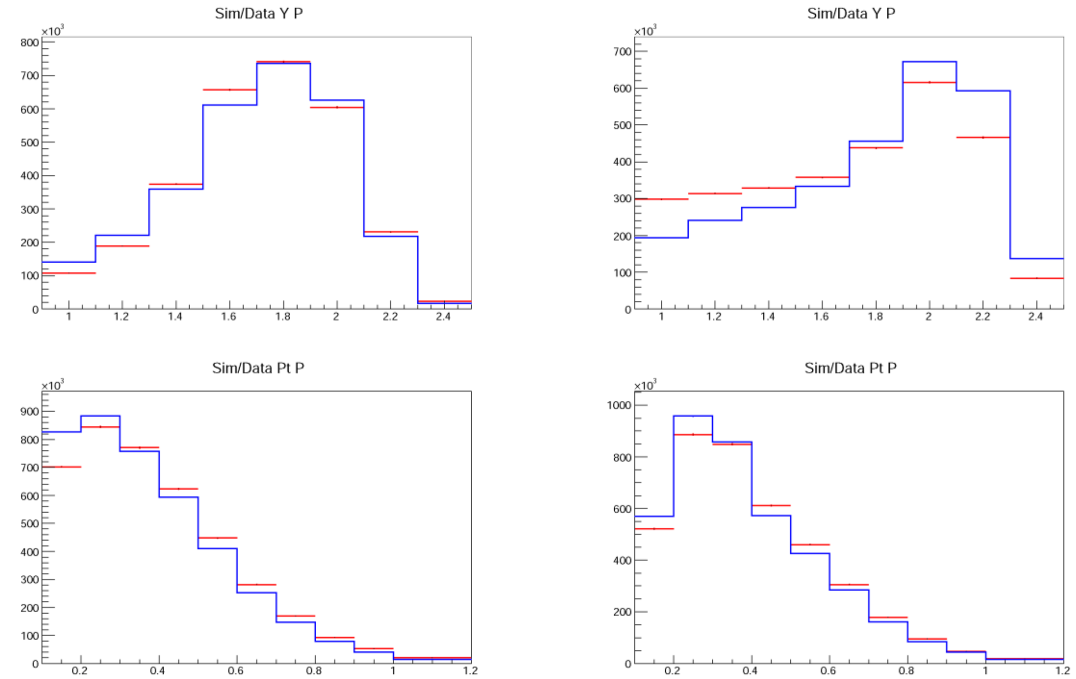

ToF-400 Sim / Data proton p_T spectrum ToF-700 Sim / Data proton p_T spectrum

Fig.11c. y_{lab} / p_T spectra of protons (upper / lower plots) identified in ToF-400 (left plots) and ToF-700 (right plots) in Ar+Sn interactions. Data are shown as red histograms, DCM-SMM simulation – as blue histograms. Simulation histograms are normalized to the data.

ToF-400 Sim / Data deuteron y spectrum ToF-700 Sim / Data deuteron y spectrum

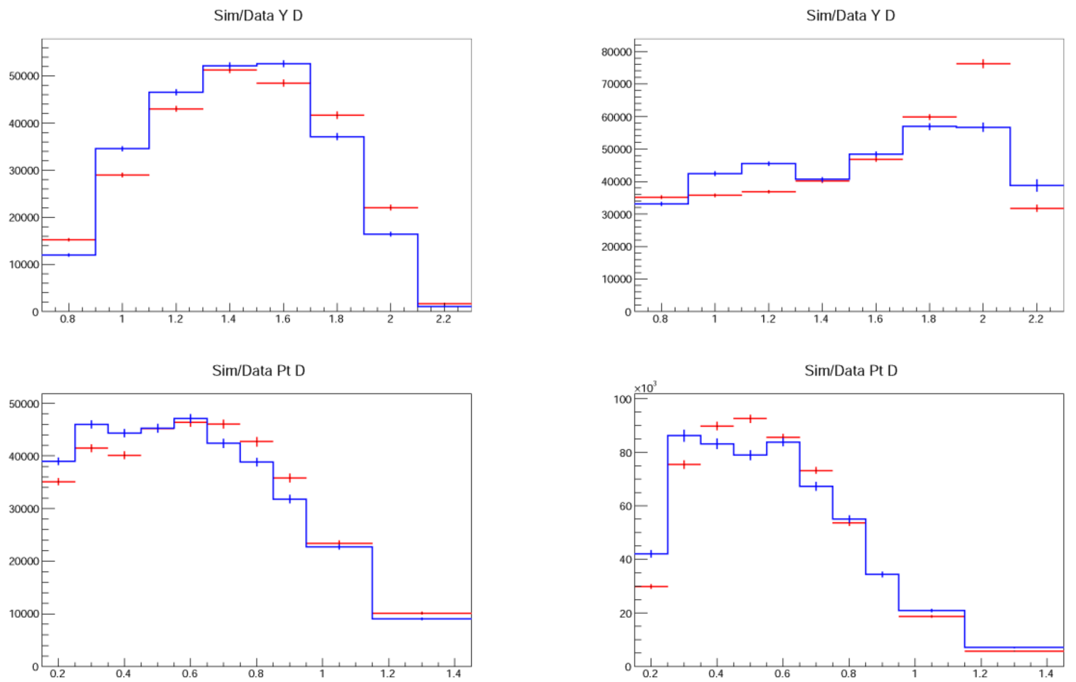

ToF-400 Sim / Data deuteron p_T spectrum ToF-700 Sim / Data deuteron p_T spectrum

Fig.11d. y_{lab} / p_T spectra of deuterons (upper / lower plots) identified in ToF-400 (left plots) and

ToF-700 (right plots) in Ar+Sn interactions. Data are shown as red histograms, DCM-SMM simulation – as blue histograms. Simulation histograms are normalized to the data.

ToF-400 Sim / Data triton y spectrum ToF-700 Sim / Data triton y spectrum

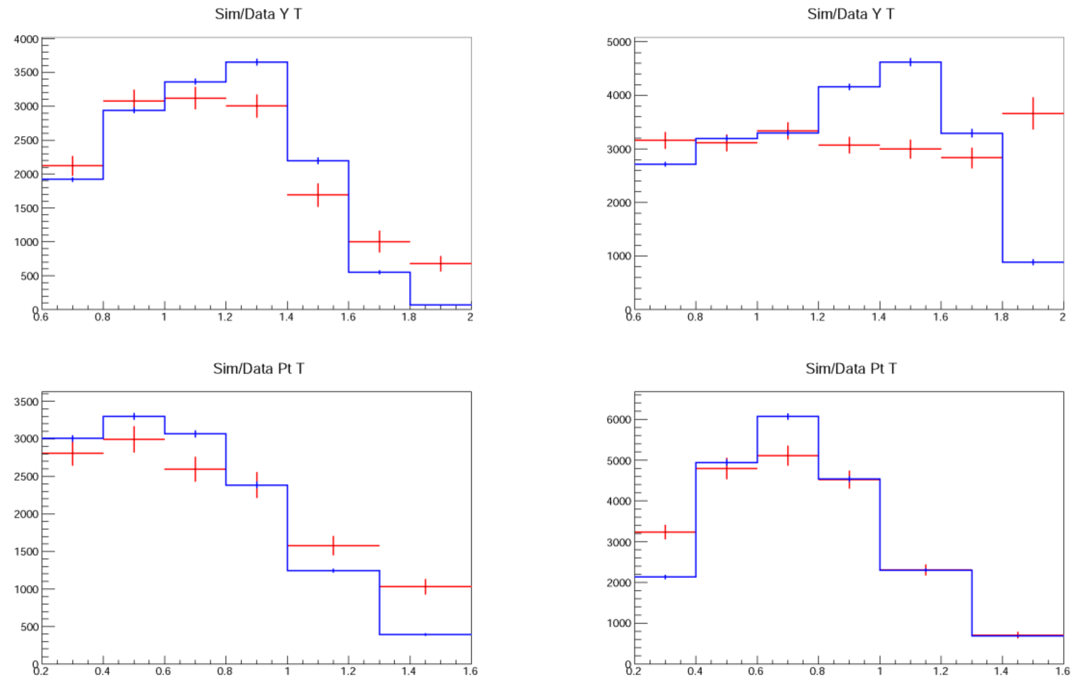

ToF-400 Sim / Data triton p_T spectrum ToF-700 Sim / Data triton p_T spectrum

Fig.11e. y_{lab} / p_T spectra (upper / lower plots) of *tritons* identified in ToF-400 (left plots) and ToF-700 (right plots) in Ar+Sn interactions. Data are shown as red histograms, DCM-SMM simulation – as blue histograms. Simulation histograms are normalized to the data.

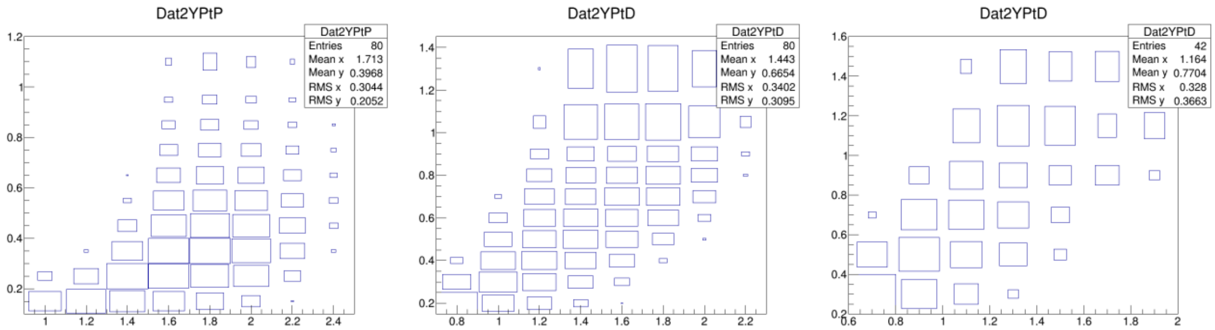

Fig.11f. Data 2-dimensional distribution of *protons (left)*, *deuterons (center)*, *tritons (right)* identified in ToF-400 in Ar+Sn interactions in bins of y_{lab} (horizontal axis) and p_T (vertical axis).

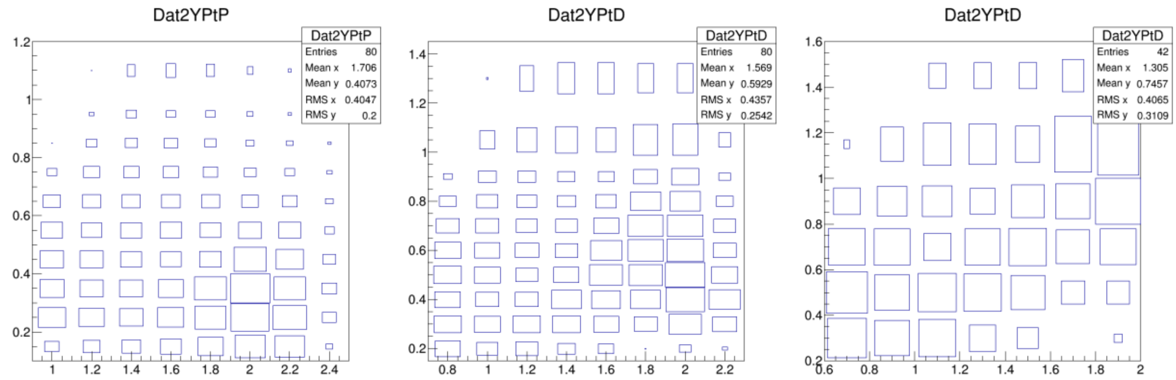

Fig.11g. Data 2-dimensional distribution of *protons (left), deuterons (center), tritons (right)* identified in ToF-700 in Ar+Sn interactions in bins of y_{lab} (horizontal axis) and p_T (vertical axis).

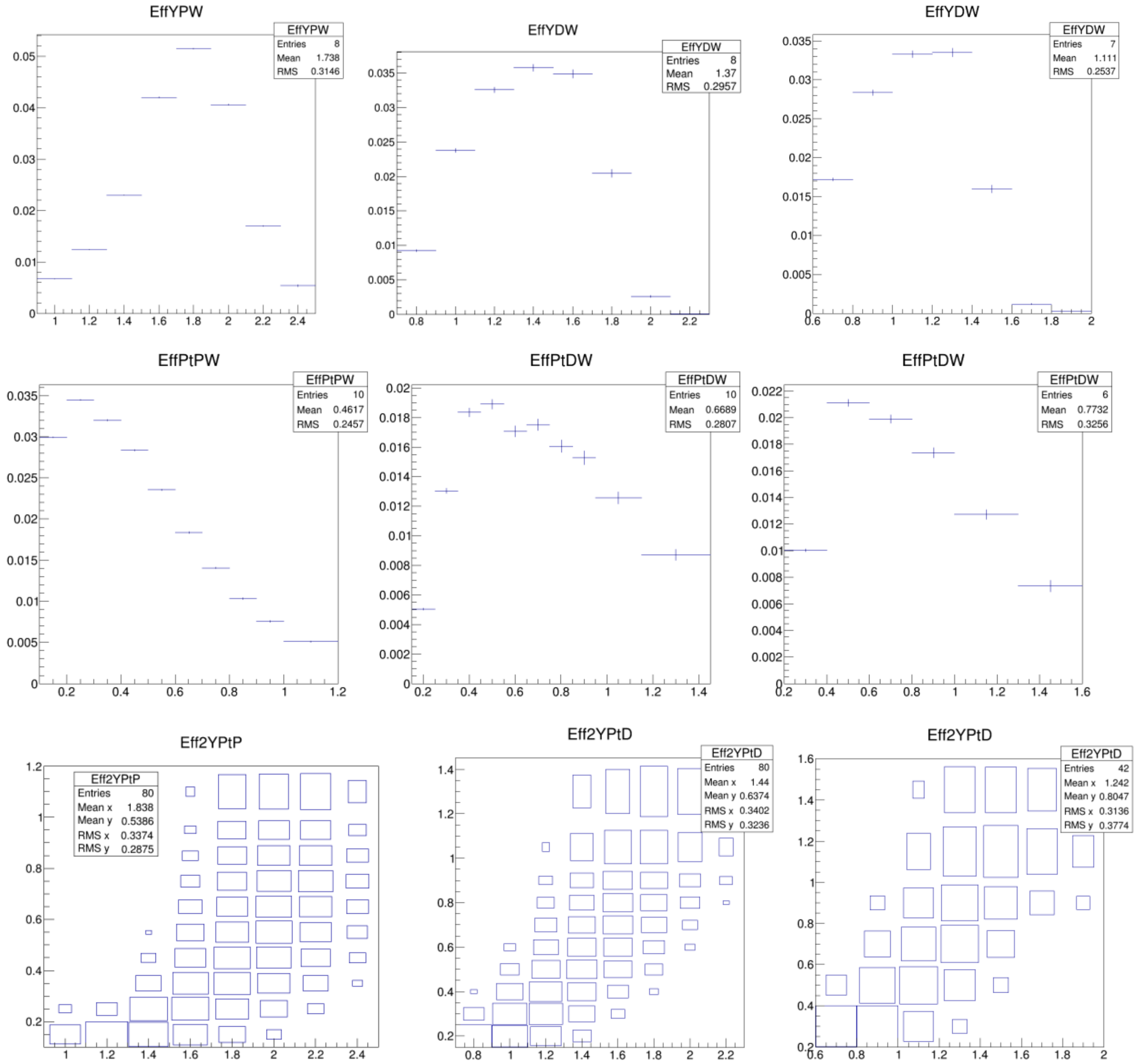

Fig.12a. Reconstruction efficiency for *protons (left), deuterons (center), tritons (right)* in bins of rapidity y_{lab} in the laboratory system (upper plots), transverse momentum p_T (center plots) and (y_{lab},p_T) – lower plots. Results are shown for particles identified in ToF-400 in Ar+Sn interactions.

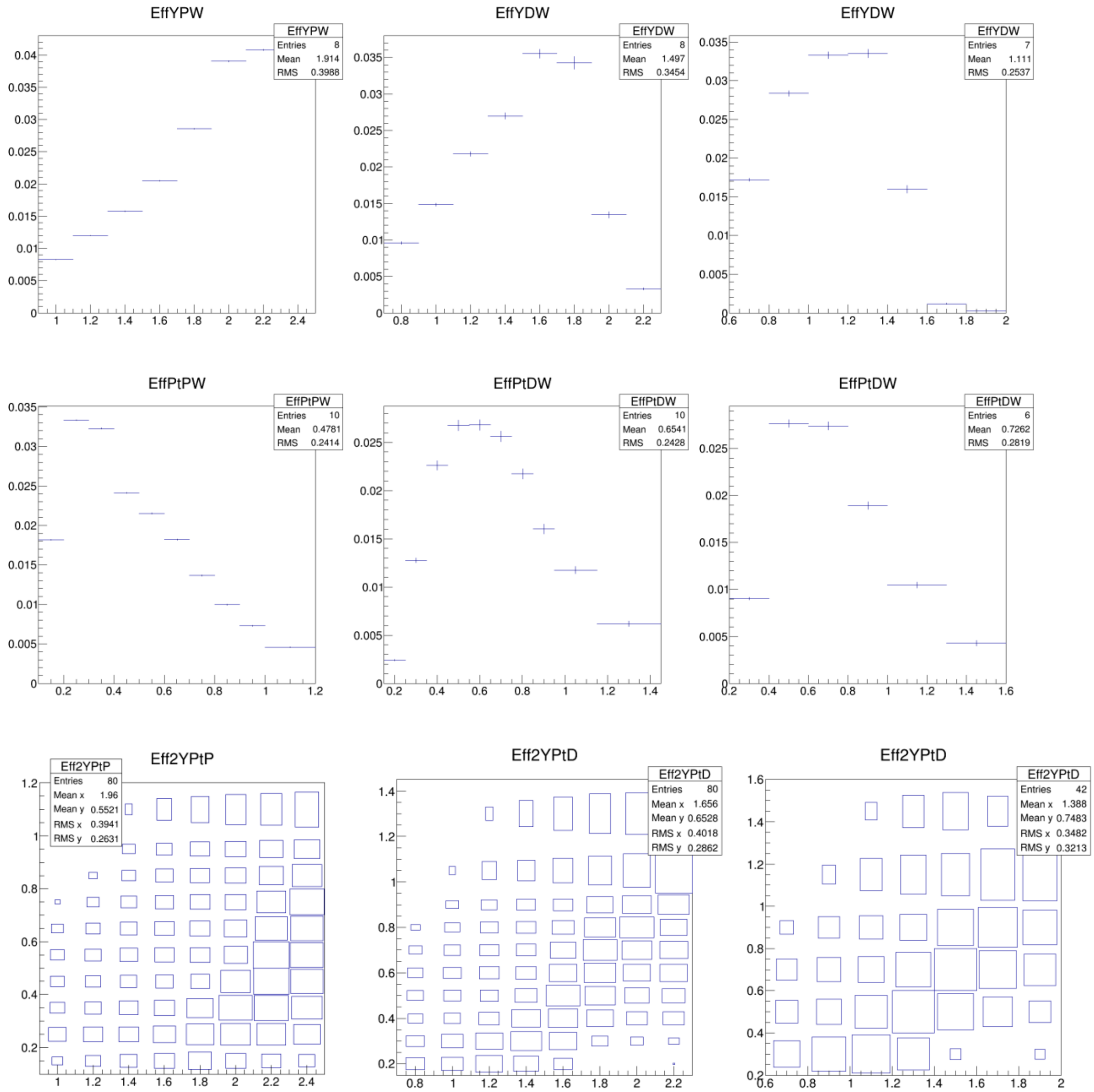

Fig.12b. Reconstruction efficiency for *protons (left)*, *deuterons (center)*, *tritons (right)* in bins of rapidity y_{lab} in the laboratory system (upper plots), transverse momentum p_T (center plots) and (y,p_T) - lower plots. Results are shown for particles identified in ToF-700 in Ar+Sn interactions.

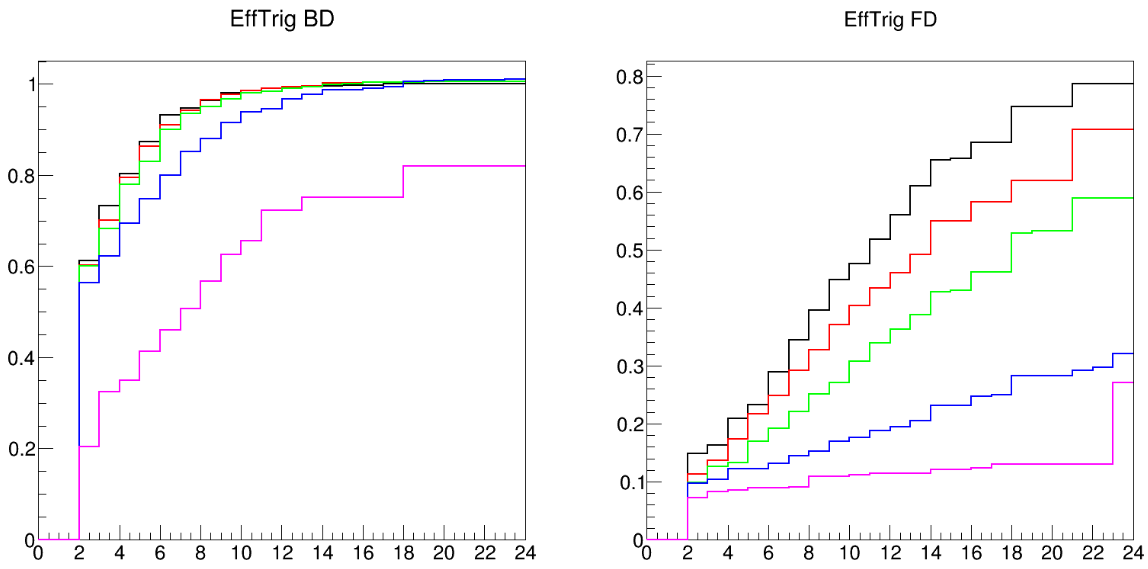

Fig.13a. BD (left plot) and SiMD (right) trigger efficiency in dependence on the number of tracks from the primary vertex calculated for interactions of the argon beam with the *C(magenta), Al(blue), Cu(green), Sn(red), Pb(black)* targets.

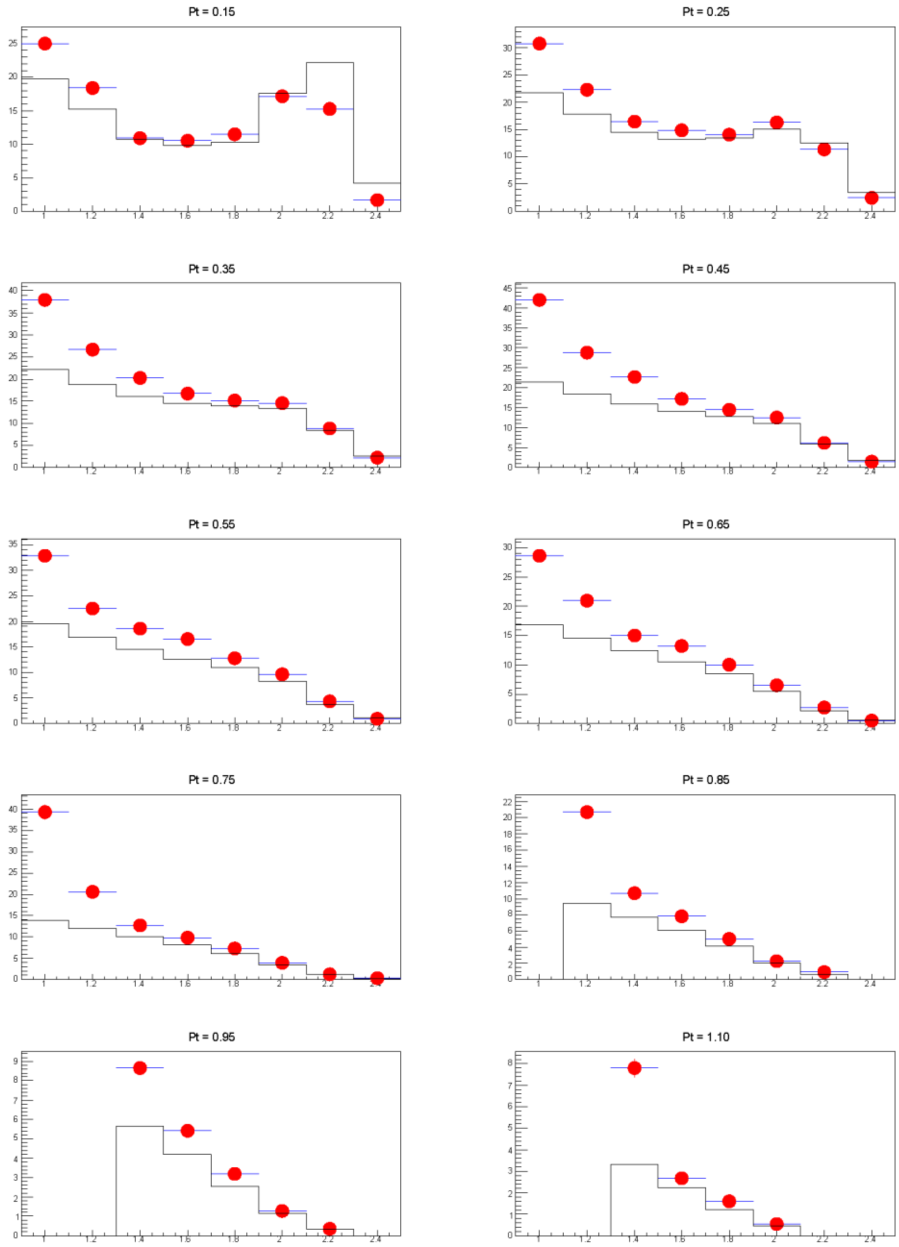

Fig15a. Reconstructed y_{lab} spectra (yields) of *protons* in *Ar+Sn* interactions with centrality 0-40%. The error bars represent the statistical errors, the boxes show the systematic errors. Predictions of the DCM-SMM model are shown as histograms.

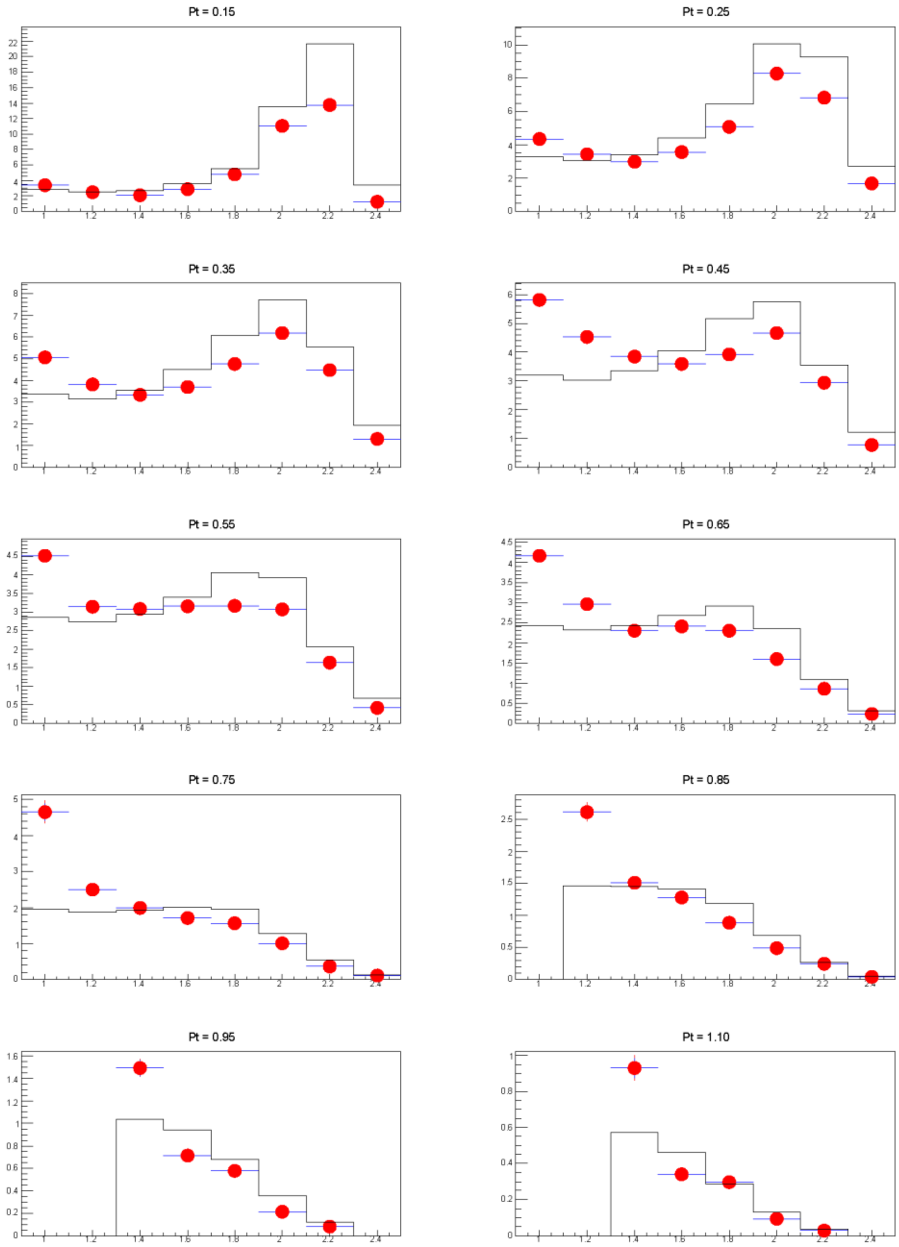

Fig15b. Reconstructed y spectra (yields) of *protons* in *Ar+Sn* interactions with centrality 40-100%. The error bars represent the statistical errors, the boxes show the systematic errors. Predictions of the DCM-SMM model are shown as histograms.

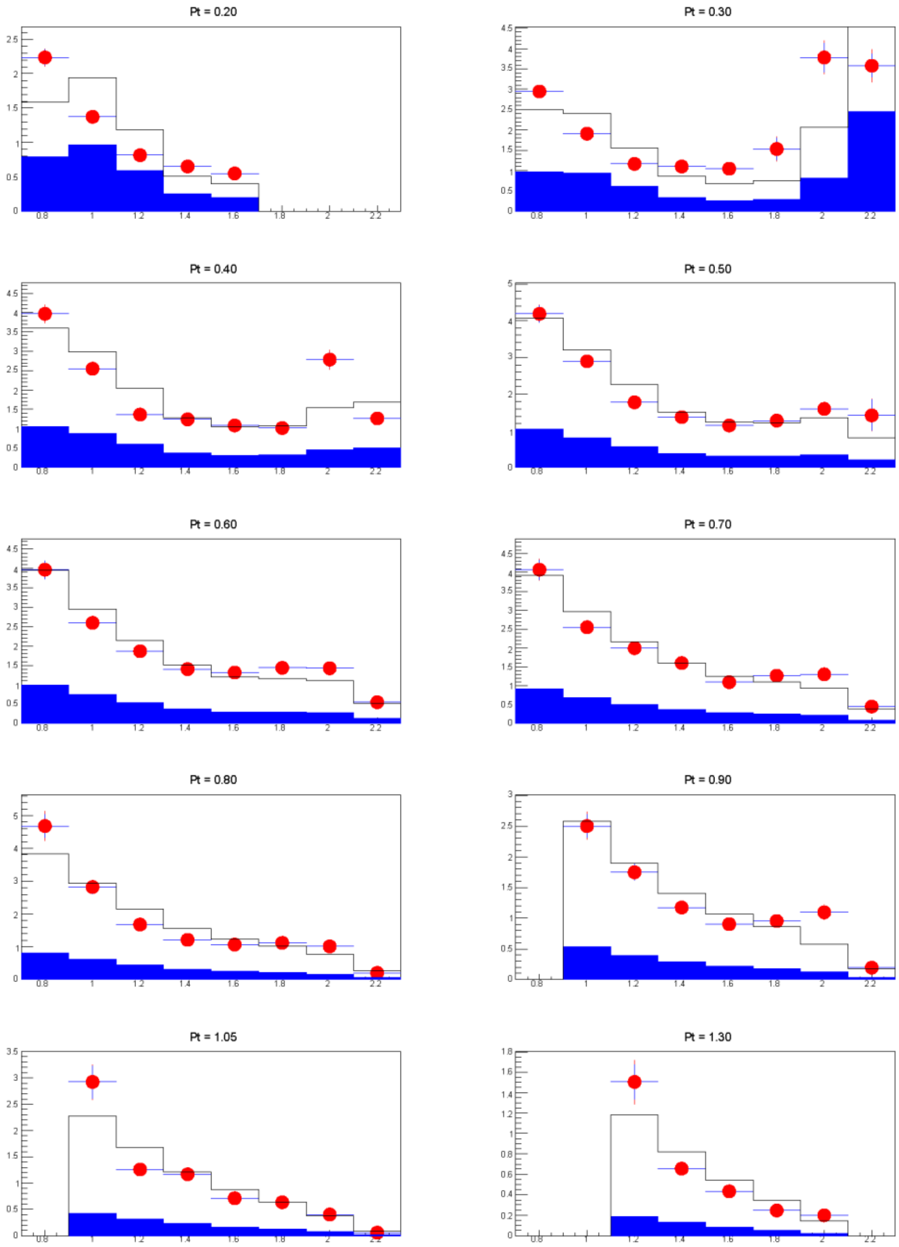

Fig15c. Reconstructed y_{lab} spectra (yields) of *deuterons* in *Ar+Sn* interactions with centrality 0-40%. The error bars represent the statistical errors, the boxes show the systematic errors. Predictions of the DCM-SMM are shown as filled histograms. Model spectra normalized to the data are presented as open histogram s.

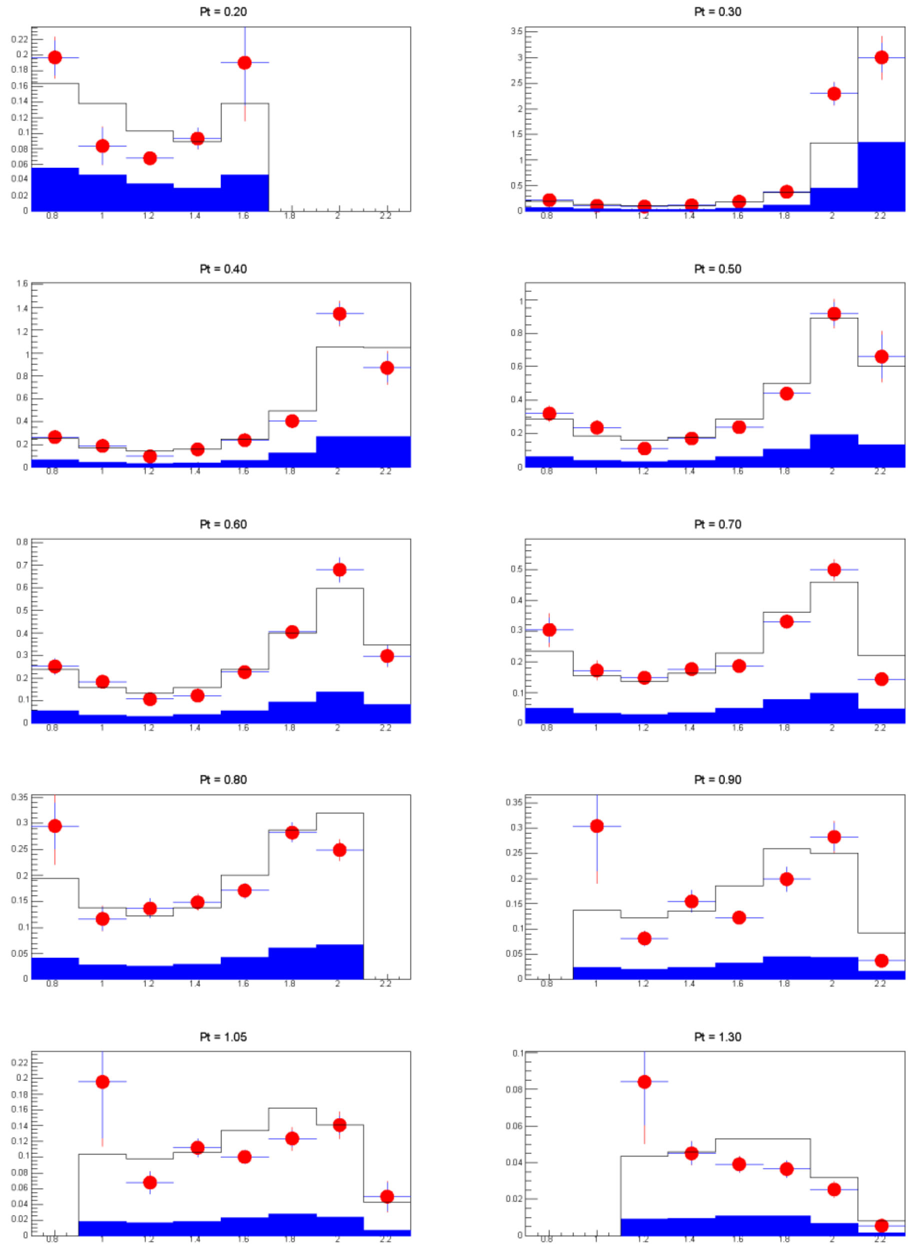

Fig15d. Reconstructed y_{lab} spectra (yields) of *deuterons* in *Ar+Sn* interactions with centrality 40-100%. The error bars represent the statistical errors, the boxes show the systematic errors. Predictions of the DCM-SMM model are shown as filled histograms. Model spectra normalized to the data are presented as open histograms.

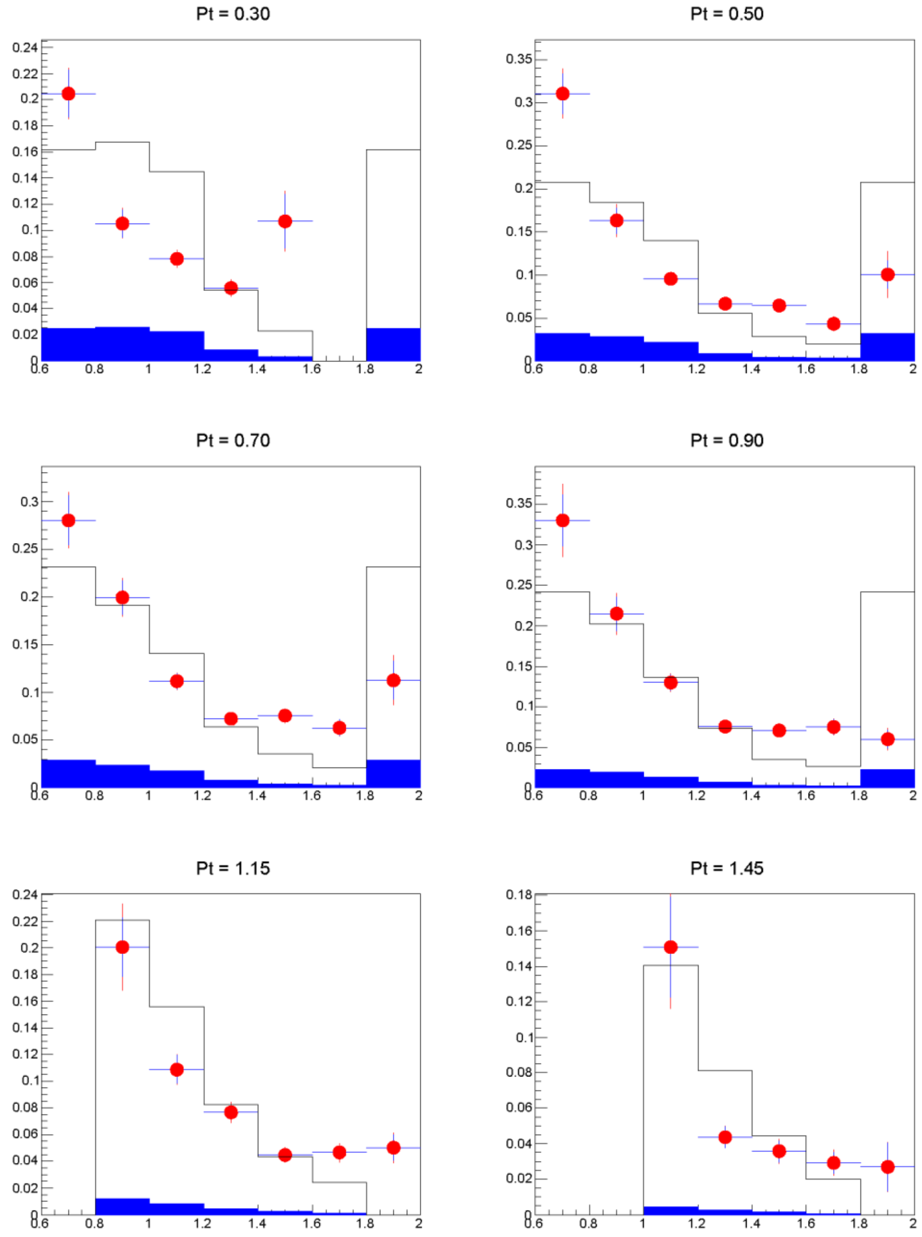

Fig15e. Reconstructed y_{lab} spectra (yields) of *tritons* in *Ar+Sn* interactions with centrality 0-40%. The error bars represent the statistical errors, the boxes show the systematic errors. Predictions of the DCM-SMM model are shown as filled histograms. Model spectra normalized to the data are presented as open histograms.

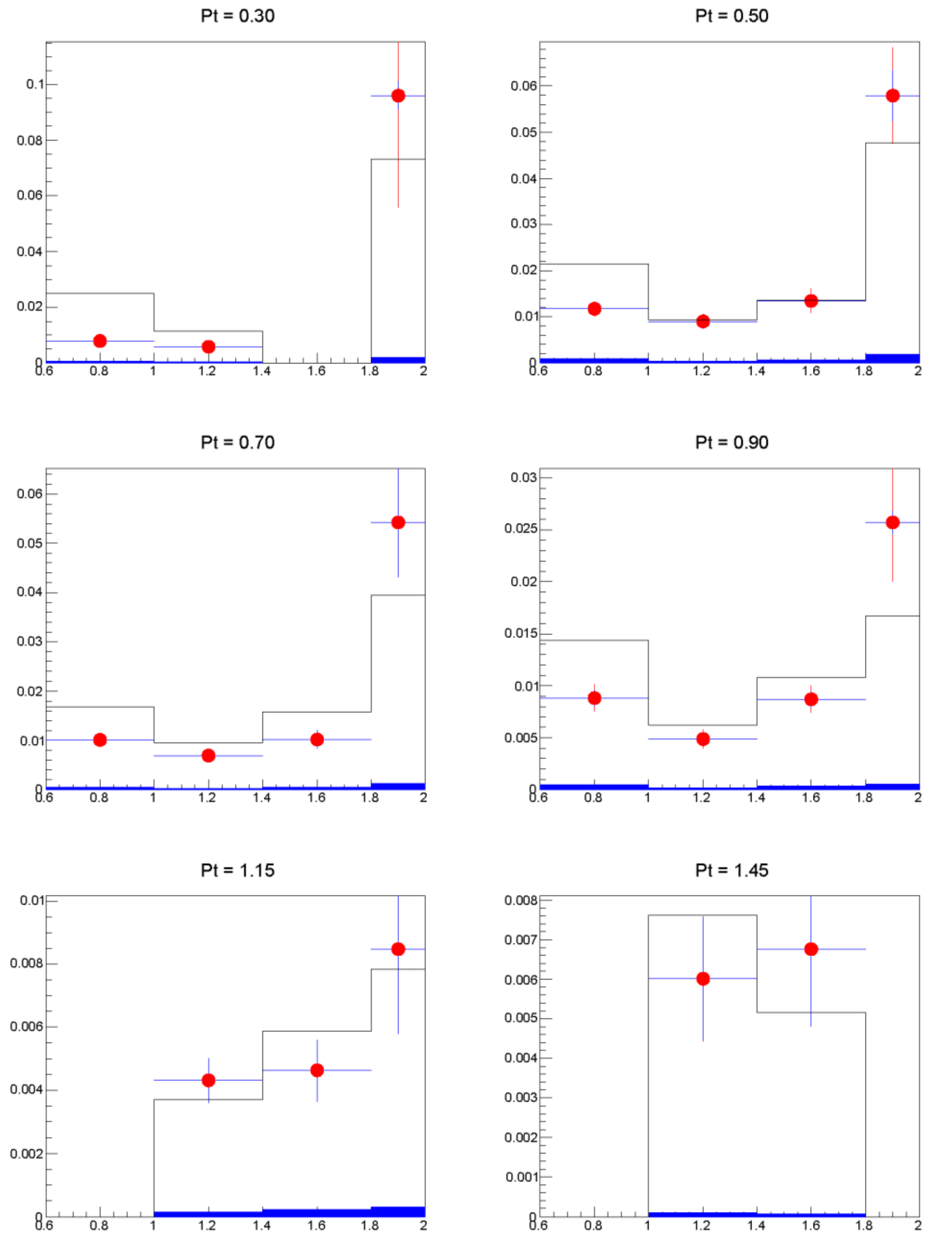

Fig15f. Reconstructed y_{lab} spectra (yields) of *tritons* in *Ar+Sn* interactions with centrality 40-100%. The error bars represent the statistical errors, the boxes show the systematic errors. Predictions of the DCM-SMM model are shown as filled histograms. Model spectra normalized to the data are presented as open histograms.

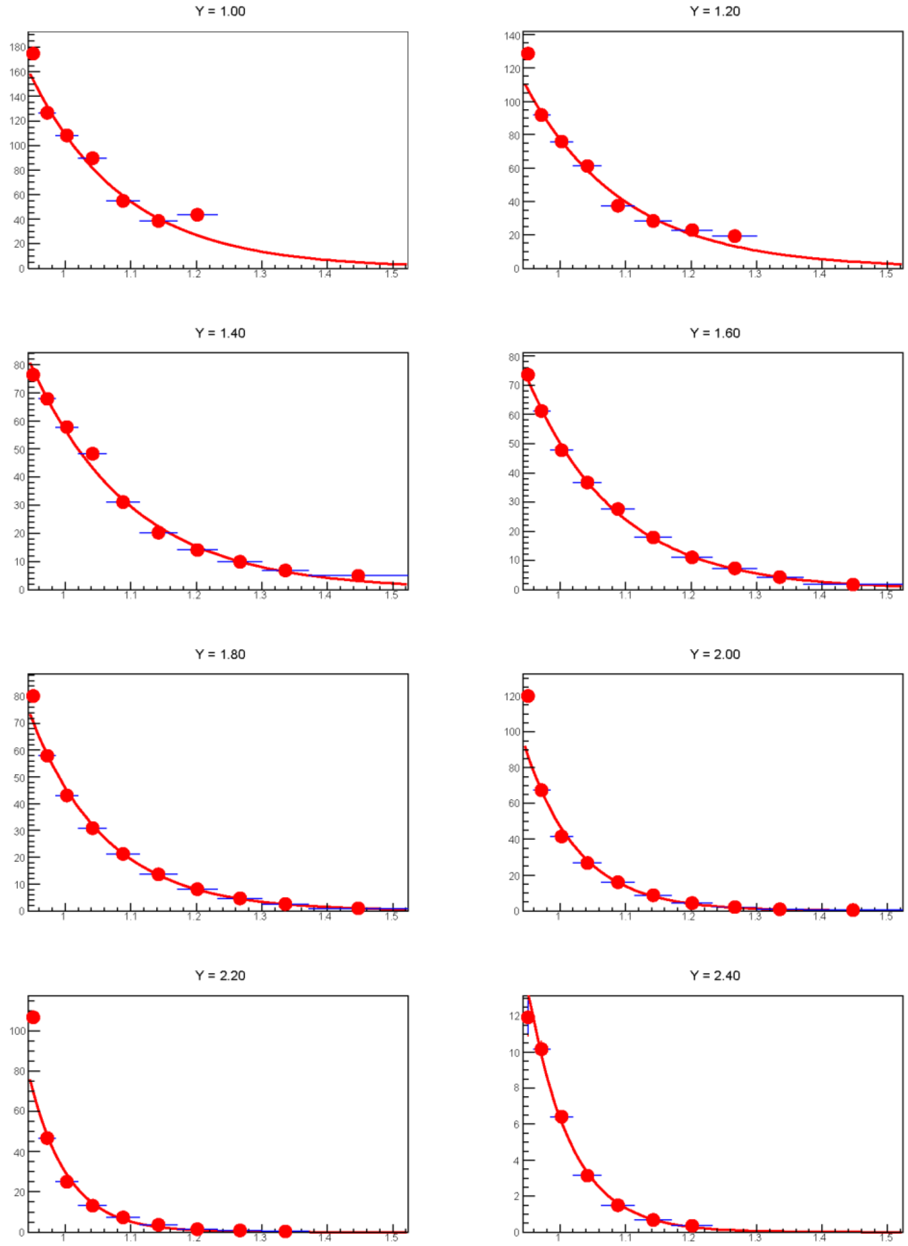

Fig.16a. Reconstructed invariant transverse momentum p_T spectra of *protons* measured in bins of rapidity y_{lab} in $Ar+Sn$ interactions with the centrality 0-40%. Results of the fit described in the text are shown as colored lines.

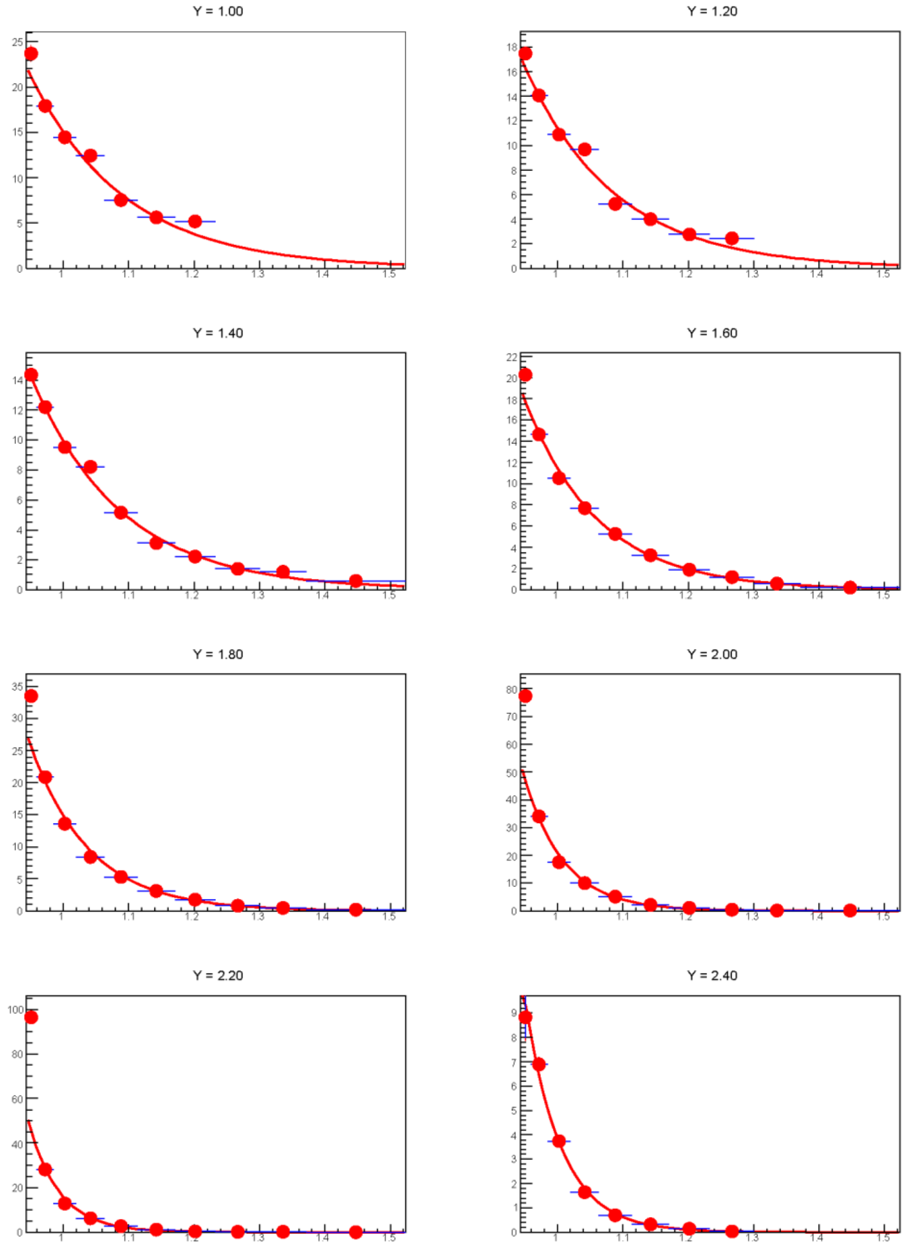

Fig.16b. Reconstructed invariant transverse momentum p_T spectra of *protons* measured in bins of rapidity y_{lab} in $Ar+Sn$ interactions with the centrality 40-100%. Results of the fit described in the text are shown as colored lines.

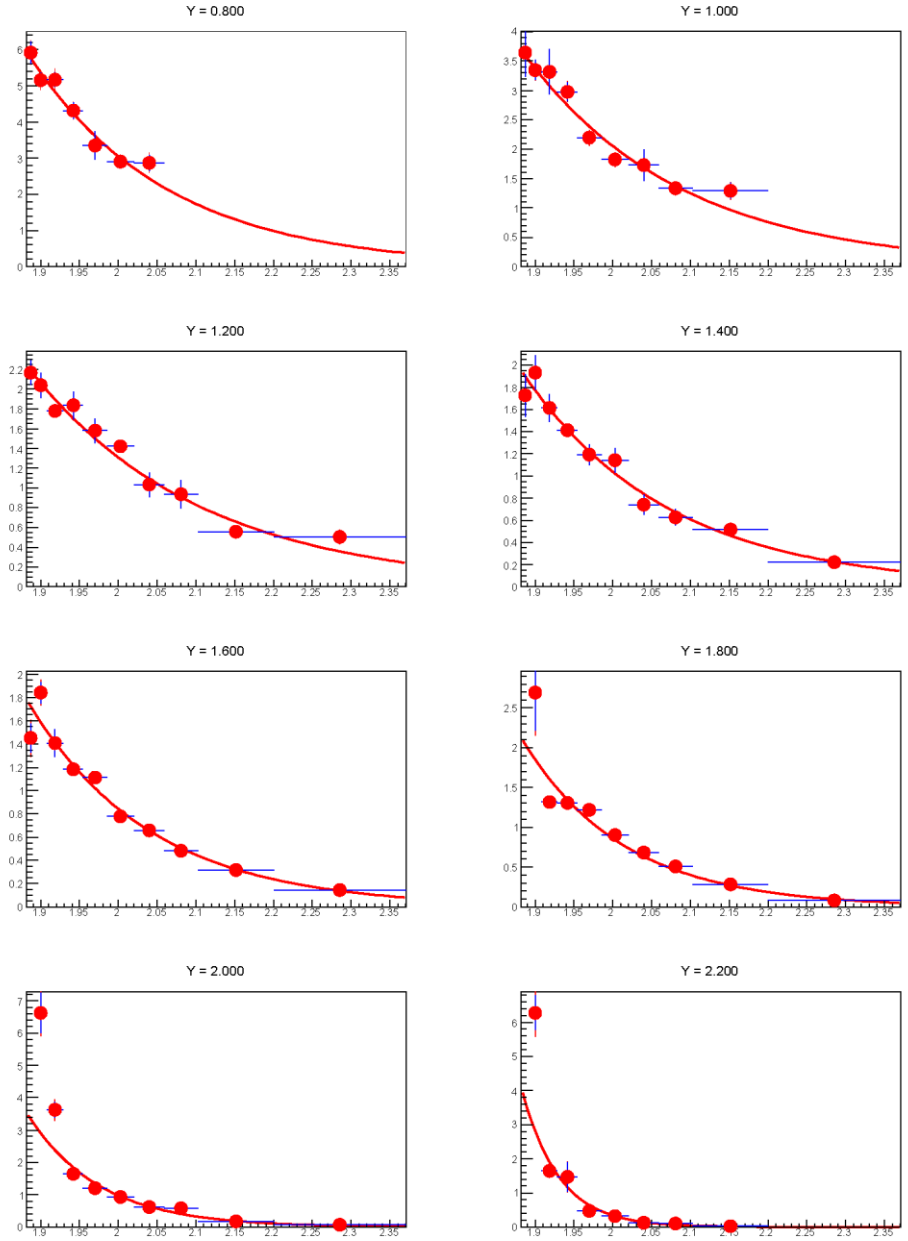

Fig.16c. Reconstructed invariant transverse momentum p_T spectra of *deuterons* measured in bins of rapidity y_{lab} in *Ar+Sn* interactions with the centrality 0-40% . Results of the fit described in the text are shown as colored lines.

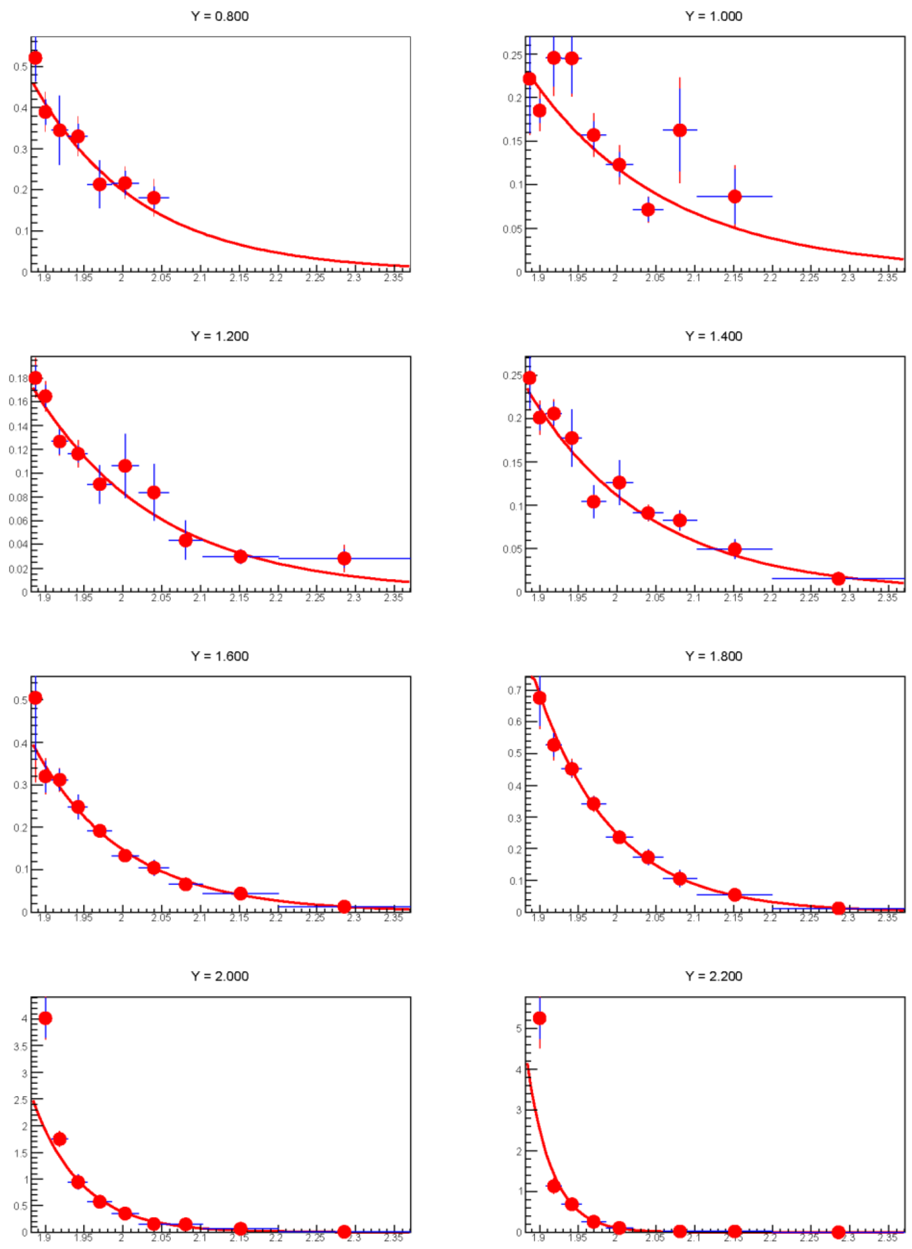

Fig.16d. Reconstructed invariant transverse momentum p_T spectra of *deuterons* measured in bins of rapidity y_{lab} in $Ar+Sn$ interactions with the centrality 40-100% . Results of the fit described in the text are shown as colored lines.

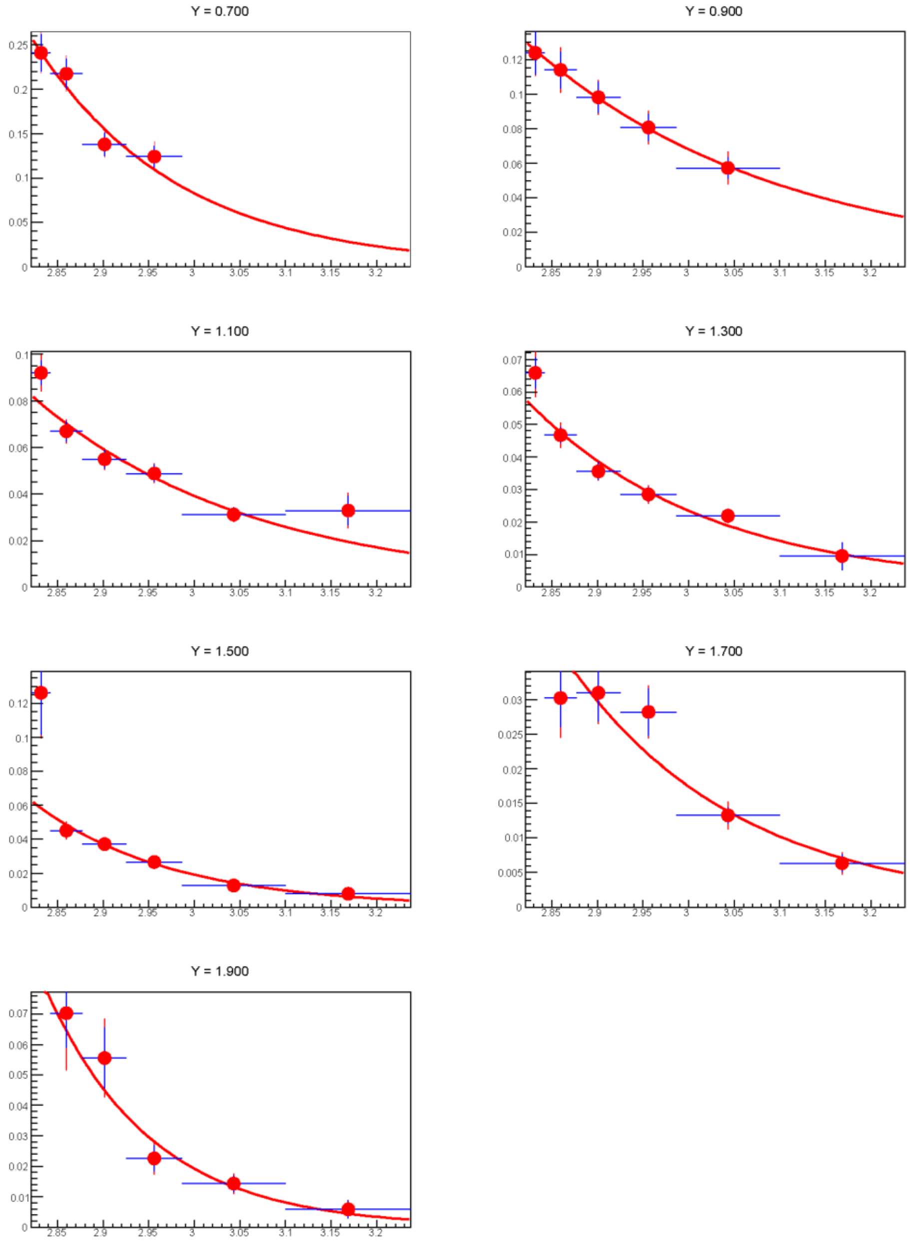

Fig.16e. Reconstructed invariant transverse momentum p_T spectra of *tritons* measured in bins of rapidity y_{lab} in $Ar+Sn$ interactions with the centrality 0-40%. Results of the fit described in the text are shown as colored lines.

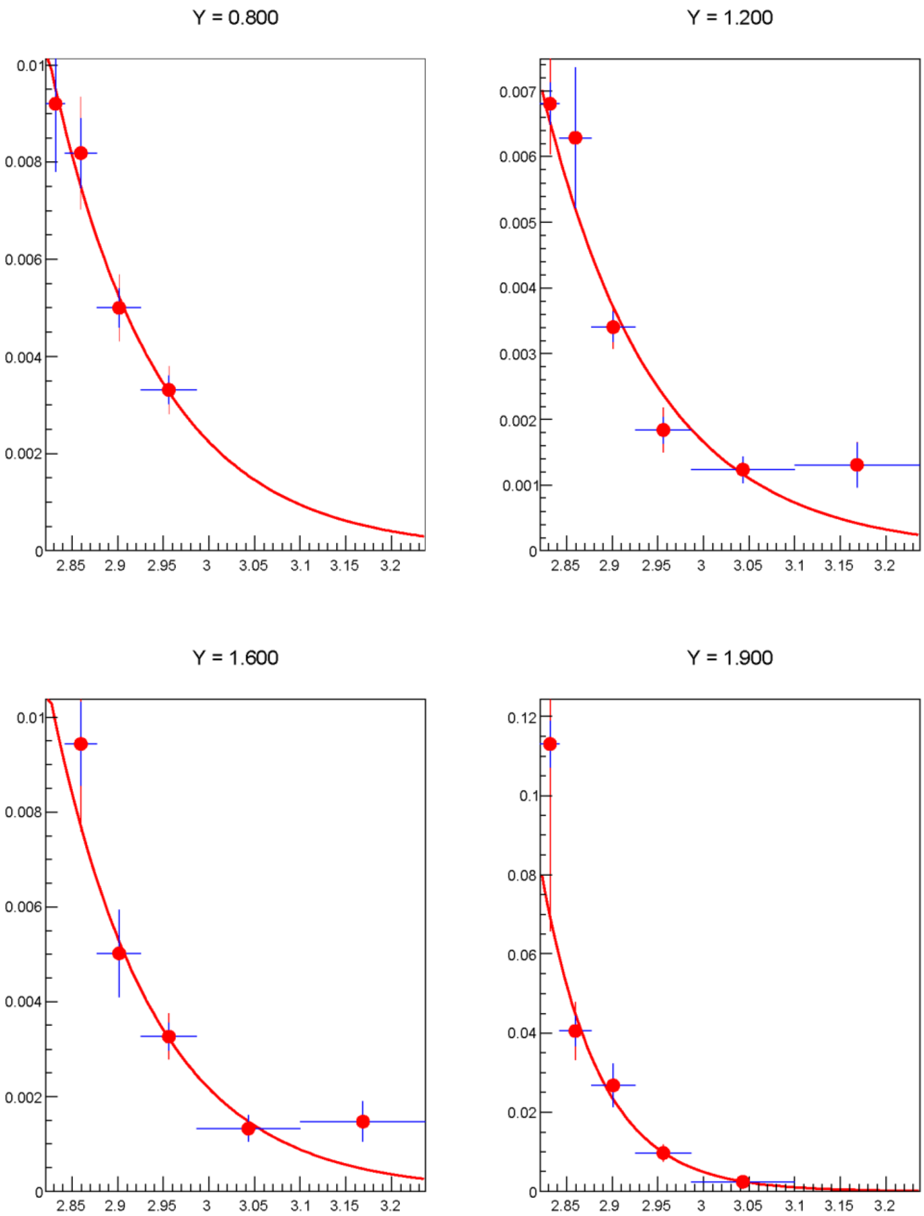

Fig.16f. Reconstructed invariant transverse momentum p_T spectra of *tritons* measured in bins of rapidity y_{lab} in *Ar+Sn* interactions with the centrality 40-100%. Results of the fit described in the text are shown as colored lines.

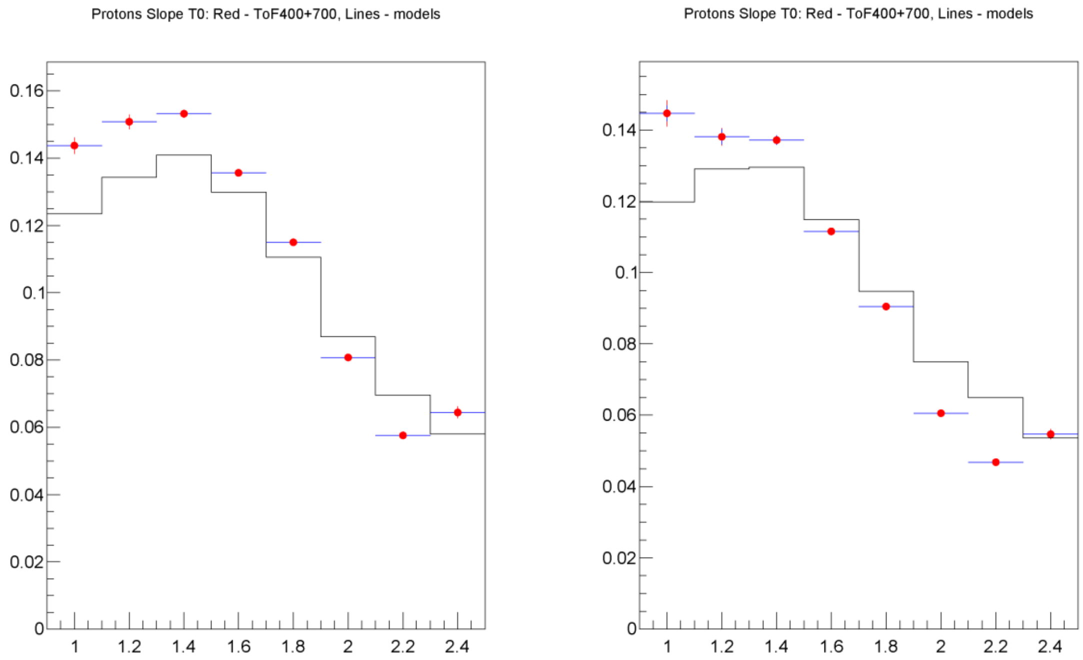

Fig17a. Inverse slope parameter T0 of the *proton* invariant p_T spectra measured in dependence on rapidity y_{lab} in *Ar+Sn* interactions with centrality 0-40% (left plot) and 40-100% (right plot). The error bars represent the statistical errors, the boxes show the systematic errors. Predictions of the DCM-SMM model are shown as a histogram.

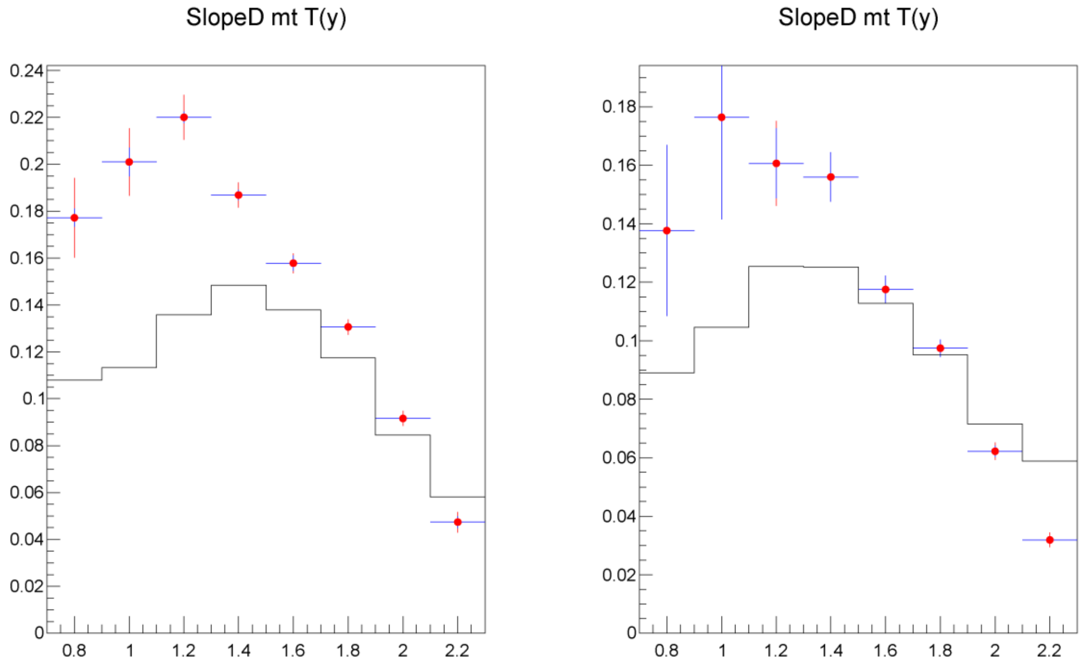

Fig17b. Inverse slope parameter T0 of the *deuteron* invariant p_T spectra measured in dependence on rapidity y_{lab} in *Ar+Sn* interactions with centrality 0-40% (left plot) and 40-100% (right plot). The error bars represent the statistical errors, the boxes show the systematic errors. Predictions of the DCM-SMM model are shown as a histogram.

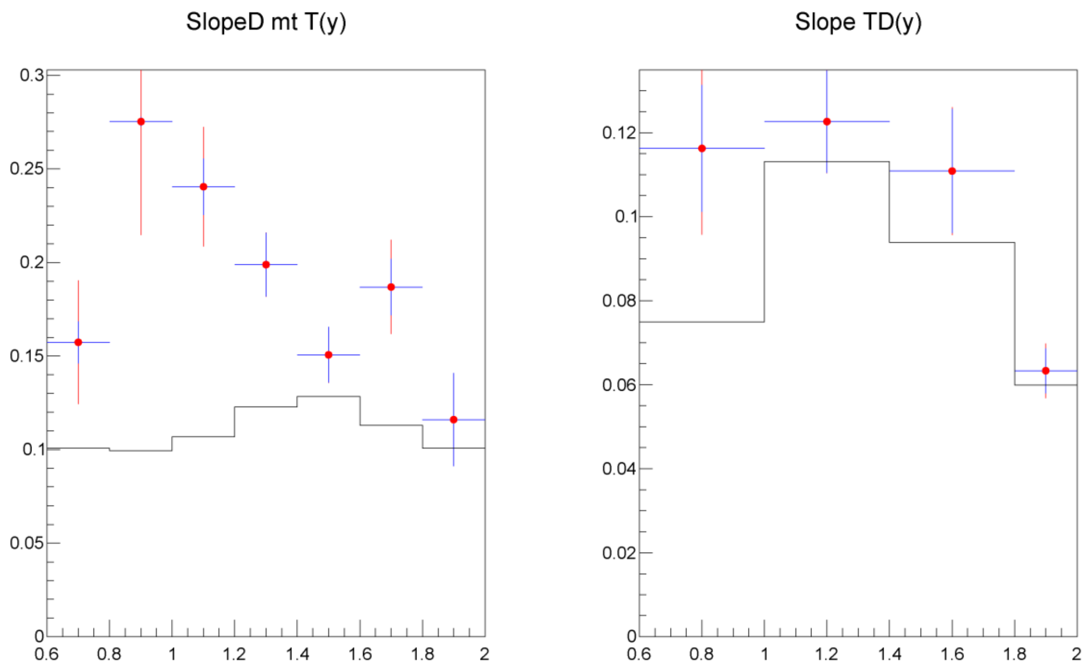

Fig17c. Inverse slope parameter T0 of the *triton* invariant p_T spectra measured in dependence on rapidity y_{lab} in *Ar+Sn* interactions with centrality 0-40% (left plot) and 40-100% (right plot). The error bars represent the statistical errors, the boxes show the systematic errors. Predictions of the DCM-SMM model are shown as a histogram.